

GEORGE R. CARRIGAN

IN-33-CR

105437

46P

F I N A L R E P O R T

Contract NAG 5-803

RESEARCH RELATIVE TO AN ADVANCED ROD CONTROL SYSTEM
FOR QUADRUPOLE MASS SPECTROMETRY APPLICATIONS

NOVEMBER, 1987

(NASA-CR-181458) RESEARCH RELATIVE TO AN
ADVANCED ROD CONTROL SYSTEM FOR QUADRUPOLE
MASS SPECTROMETRY APPLICATIONS Final Report
(Michigan Univ.) 46 p Avail: NTIS HC
A03/MF A01

N88-11050

Unclas

CSCL 09A G3/33 0105437

George R. Carrigan
The University of Michigan
Space Physics Research Lab
2455 Hayward
Ann Arbor, Michigan 48109-2143

November, 1987

Final Report

NAG 5-803

Research Relative to an Advanced Rod Control System
for Quadrupole Mass Spectrometry Applications

The University of Michigan was funded under a NASA Grant, NAG 5-803 to investigate an improved RF oscillator design for quadrupole mass spectrometers routinely used by Goddard Space Flight Center in flight applications.

The work under the grant has been successfully completed and two suitable options for the next flight opportunity have been identified and studied. The development of the oscillator will continue as part of the definition study for the CRAF mission. The work under NAG 5-803 has been fully documented in two reports that are appended hereto. This cover and the two reports are submitted to satisfy the requirement for a Final Technical Report.

Appendix I Advanced Rod Control System Feasibility Study
Appendix II Three Frequency Oscillator Tank Circuit

ADVANCED ROD CONTROL SYSTEM FEASIBILITY STUDY

Alan B. Macnee
August 15, 1986

University of Michigan

To: Bruce P. Block

August 15, 1986

From: Alan B. Macnee

Subject: Advanced Rod Control System feasibility study

The Advanced Rod Control System outlined by Bruce Block in his September 20, 1985 proposal includes a broadband linear amplifier to drive the quadrupole mass spectrometer rods. The proposed amplifier should produce a 350 volt peak-to-peak sine wave across the rod pairs over the frequency range of 0.5 to 15 Mhz. This report summarizes the results of my investigations into the design of a suitable amplifier output stage using available transistors and passive components.

1. Introduction

A block diagram of an amplifier and quadrupole load is given in Fig. 1.

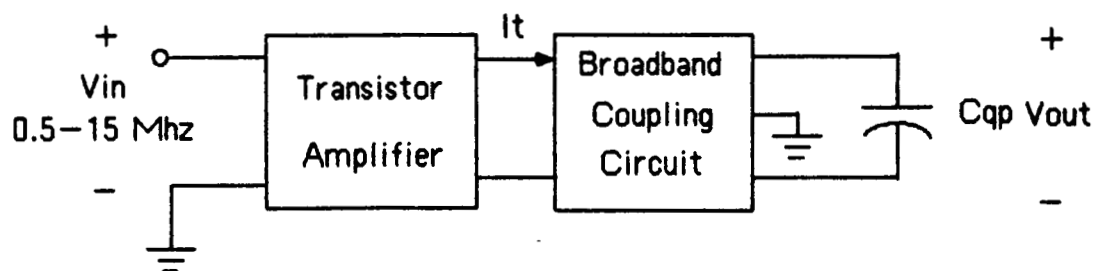


Fig.1 Amplifier and quadrupole load.

The quadrupole load can be represented for design purposes by a 25 picofarad capacitance which is balanced with respect to the signal ground. This represents the capacitance between the two pole pairs plus one half of the capacitance from either pole pair to ground. To a first approximation the transistor amplifier can be expected to act as a constant current source. The broadband coupling circuit should therefore have a constant transfer impedance over the frequency range $0.5-15 \text{ Mhz}$. Physical realizability considerations for the coupling circuit, with the capacitive load plus the needed voltage swing, sets a lower bound on the power that must be supplied by the transistor amplifier. That limit is presented in the next section. It is followed by some preliminary amplifier design and simulation in Section 3.

2. Coupling Circuit Design

The 30:1 frequency range required means that the coupling circuit is essentially a lowpass design. Placing a shunt resistor at the input end, the problem is to select a lowpass circuit to give an almost constant transfer impedance

$$|V_{out}/I_t| = |Z_{21}(jf)| \text{ for } 0 < f < f_{max}.$$

For a passive, reciprocal coupling circuit, the positions of the current excitation and the voltage output can be interchanged as indicated in Fig.2 .

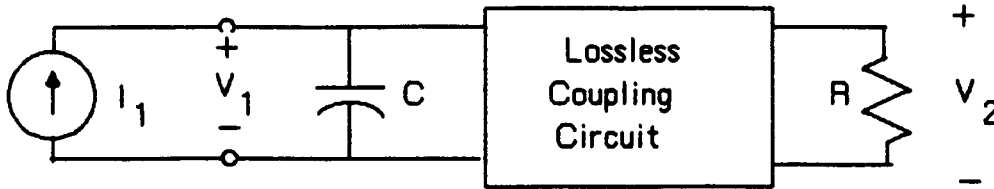


Fig.2 Equivalent Coupling Circuit.

In this equivalent, the coupling circuit is assumed lossless since this will lead to the minimum power required from the current source (transistor amplifier). The limitation imposed on this circuit was developed by H. Bode . The resistance seen by the current source is restricted by the requirement that

$$\int_0^{\infty} R_1(2\pi f) d(2\pi f) = \frac{\pi}{2C} \quad (1)$$

where

$$R_1(j2\pi f) = \text{Real} \{ V_1/I_1 \}. \quad (2)$$

Equation (1) is known as the Bode Resistance integral. Bode recognized the importance of this integral in the design of input or output coupling circuits ¹.

1. H. Bode; Network Analysis and Feedback Amplifier Design; d. van Nostrand & Co.; New York; 1945; Chapter 16.

As long as the coupling circuit is lossless, the average power supplied by the current source I_1 is all delivered to the resistor R . Therefore

$$|I_1|^2 * R_1 = |V_2|^2 / R = P_{avg} \quad (3)$$

or

$$|V_2/I_1| = |Z_{21}| = \sqrt{R_1 * R}. \quad (4)$$

For a lowpass design, one would like to have $R_1=R$ for $0 < f < f_{max}$. Assuming in the ideal case, that this goal can be achieved, Eq.(1) requires that

$$R * f_{max} * 4C = 1. \quad (5)$$

and the average power supplied to the resistor R will be

$$P_{avg} = |V_{2max}|^2 / 8R \cong 0.5 * |V_{2max}|^2 * f_{max} * C \quad (6)$$

where

P_{avg} = power supplied to coupling circuit

V_{2max} = peak-to-peak voltage across C

f_{max} = highest frequency in Hertz.

This is the minimum average power that must be supplied by the current source to achieve a constant voltage across the capacitance C from 0 to f_{max} . Practical coupling circuits can come very close to this limit.

Normalized lowpass coupling circuit designs can be found in many network texts and handbooks.² For instance Weinberg's Table 13-4 for 0.5db Chebyshev designs gives $C=1.5982$ farads for $R=1$ ohm and $f_{max} = 0.1592$ Hertz for a 7 pole filter. This is within 1.3% of the limit set by Eq.(5)! Impedance and frequency scaling to make $C=25$ pF and $f_{max}=15$ Mhz gives $R=678.5\Omega$ for the Chebyshev design versus 666.7Ω for the Bode limit of Eq.(5).

² L. Weinberg; Network Analysis and Synthesis; McGraw-Hill; New York; 1962; Chapter 13.

Figure 3 gives the element values of this scaled Chebyshev design .

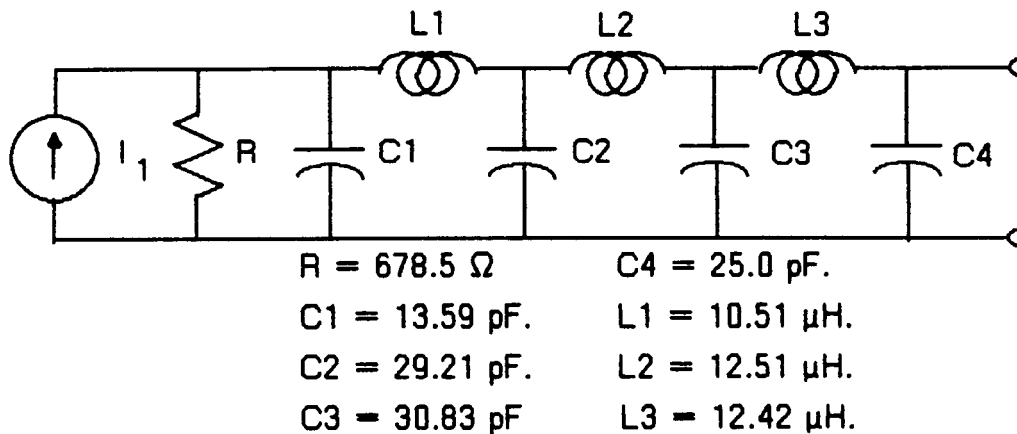


Fig. 3 Chebyshev lowpass filter, 0.5 db ripple, $f_{max}=15$ Mhz.

For 350 volts peak-to-peak across C4, I_1 must be 0.5158 amps. peak-to-peak, and the average power supplied by the current source (transistor amplifier) must be 22.57 watts. The next section investigates the design of a push-pull class B transistor amplifier to supply this power and voltage swing. It should be borne in mind that the average power requirement depends directly on the choices of the quadrupole voltage V_{2max} and the highest frequency f_{max} (See

Eq.(6)). If for instance these were reduced to 250 volts p-p and 10Mhz, the required power would drop to 7.68 watts!

It also should be noted that the magnitude of the input impedance "seen by" the current source in Fig.3 varies between 678.5 and zero ohms; however as long as the current source is held constant the specified equal-ripple transfer impedance will be achieved.

The voltage swing required across L_1 in Fig.3 is too large to be produced by typical high-frequency, bipolar, power transistors. This can be reduced by the introduction of input transformer, which also is convenient for a push-pull class B driver amplifier. Figure 4 shows the circuit of Fig.3 with a transformer added.

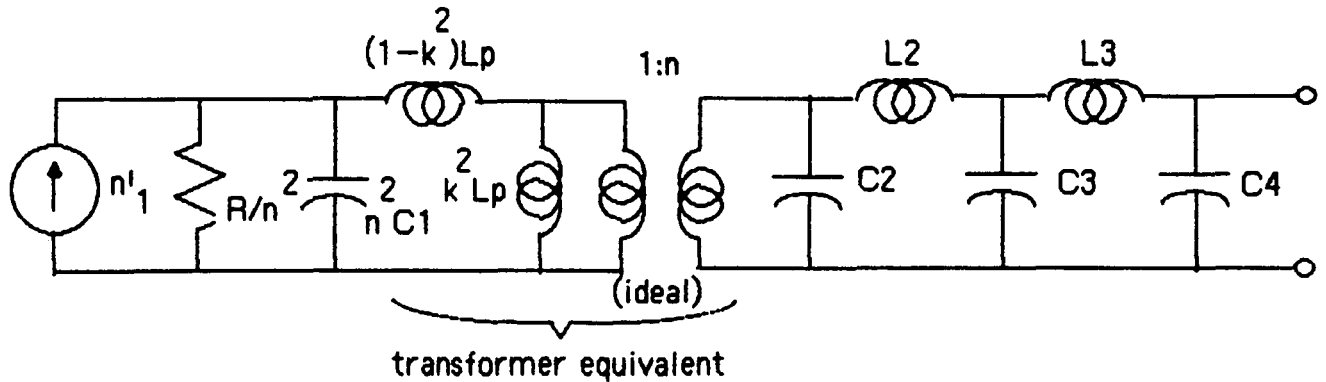


Fig. 4 Equivalent circuit of lowpass filter plus transformer

In this circuit the coupled coils of the transformer have been replaced by an ideal transformer, the magnetizing inductance $k^2 L_p$ and the leakage inductance $L_p(1-k^2)$. Transformer losses and stray capacitances are not included. Choosing the leakage inductance equal to L_1/n^2 should preserve the high-frequency performance of the Fig.3 low-pass design .

$$L_p(1-k^2) = L_1/n^2 \quad (7)$$

Further, the lower half power frequency will be approximately

$$f_{low} = R/(n^2 2\pi k^2 L_p) \quad (8)$$

Eliminating k between (7) and (8) gives an equation for L_p

$$L_p = (L_1 + R/(2\pi f_{low})) / n^2 \quad (9)$$

where

L_1 is the first inductance in Fig.3

R is the shunt resistance before transformation

f_{low} is the desired lower half power frequency in Hertz, and

n is the chosen impedance transformation.

Having used (9) to find L_p , Eq.(7) can be solved for the required coefficient of coupling. An alternative approach is to select n and k ; use (7) to find L_p ; and then (8) gives the lower half power frequency that can be achieved.

As an example, choosing $n=4$ and $f_{low}=0.5\text{Mhz}$ for the circuit of Fig.4, one finds that L_p must be $14.16\mu\text{H}$ and the coefficient of coupling must be 0.9765 . In this design then, $n^2C_1=217.4\text{pF}$, $(1-k^2)L_p=0.6569\mu\text{H}$, $k^2L_p=13.5\mu\text{H}$, and $R/n^2=42.4\Omega$. The peak-to-peak input current required is now increased to 2.063 amperes for 350 volts p-p across C_4 .

The calculated frequency response of the example design is shown in Fig.5.

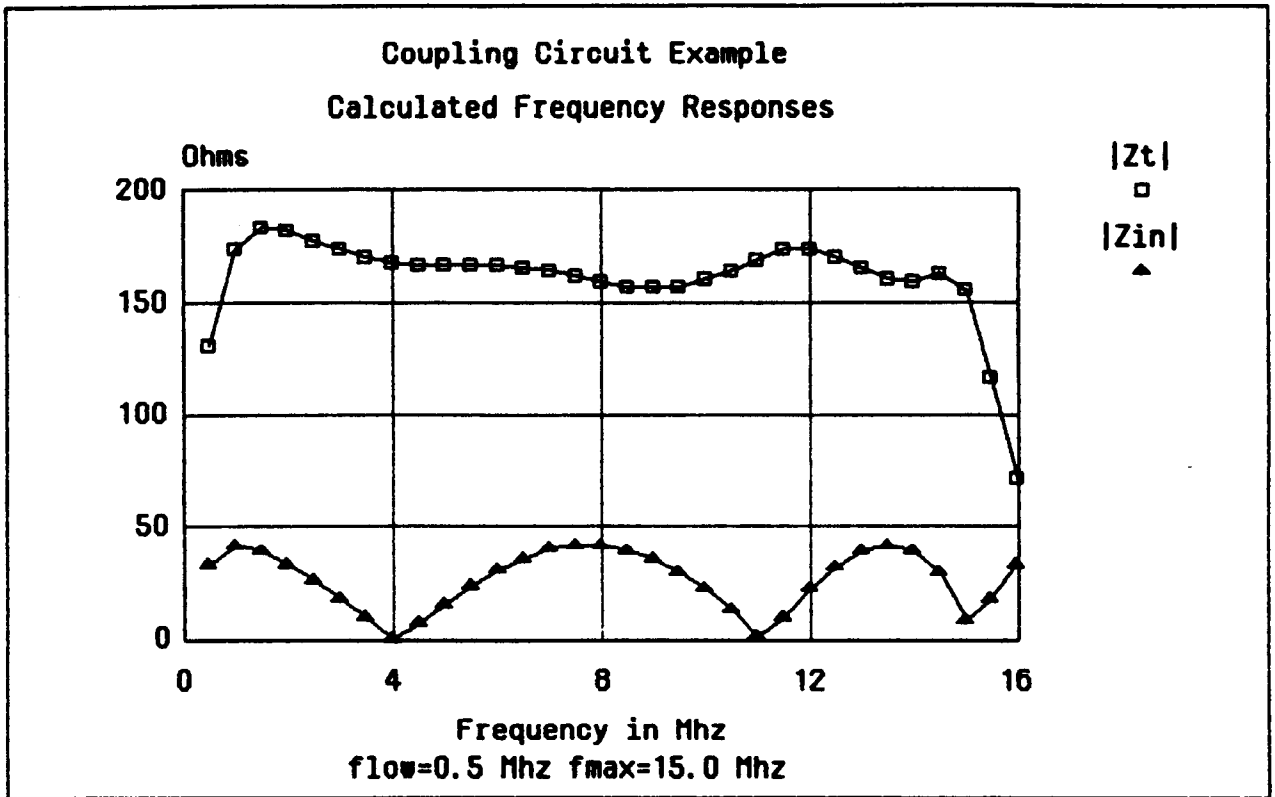


Fig.5 Input and Transfer Impedance magnitudes for Fig.4

From 3.5 to 15 Mhz the transfer impedance is close to the Chebyshev prototype design, which would oscillate between 160.1 and 169.6 ohms. The transformer magnetizing inductance causes the peak of 182.9Ω at 1.5Mhz followed by the drop to 131.3Ω at 0.5Mhz . The magnitude of the input impedance oscillates between zero and 42.4 ohms as expected.

3. Amplifier Design

To furnish a sinusoidal current excitation to the lowpass transformer coupled circuit (Fig.4) a class B , push-pull circuit was chosen because of its potential efficiency. For initial design calculations $2\text{N}5102$ transistors were assumed. This transistor type has been used in earlier quadrupole oscillator driver

circuits, and therefore we have reasonable large signal models for use in the SPICE simulations. The basic amplifier circuit is given in Fig.6 .

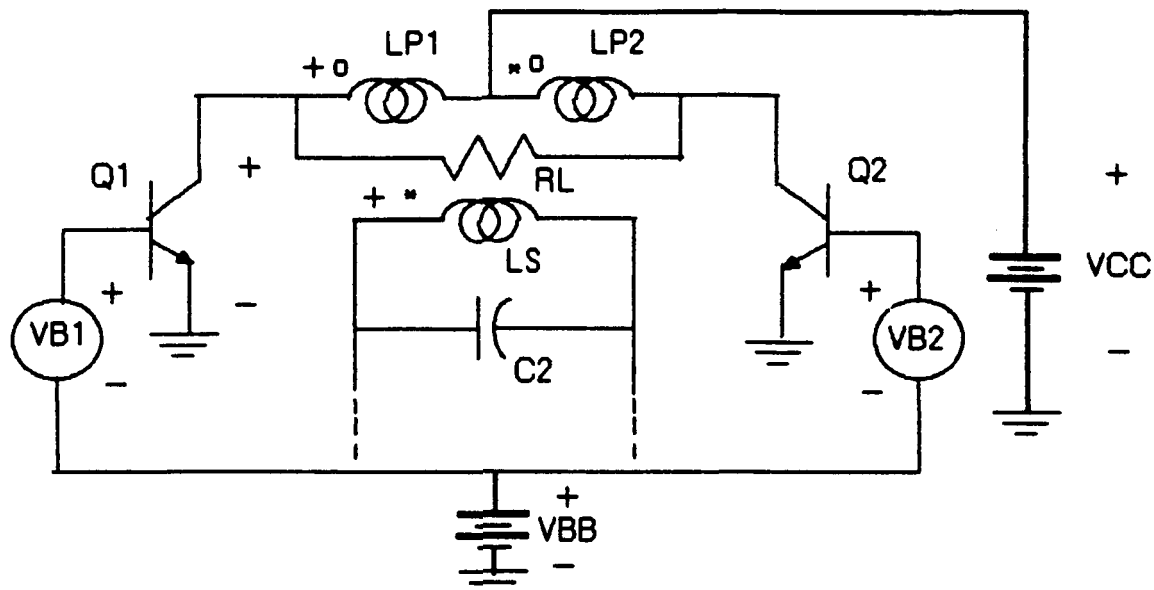


Fig.6 Push-pull quadrupole amplifier circuit

In this figure the portion of the coupling circuit beyond C2 has not been drawn (see Fig.4). The two primary windings are the result of center tapping the primary in Fig.4 so that the load impedance for each transistor varies between $42.4 \div 4 = 10.6 \Omega$ and zero depending upon the frequency. The shunt input capacitance $n^2 C1$ is replaced by the transistor output capacitances. The initial SPICE simulations were made without an additional capacitance, but my present conclusion is that capacitance will have to be added to give the desired transfer impedance.

For these initial amplifier simulations the secondary inductance was $LS = k^2 n^2 Lp = 216 \mu H$, the primary inductances were $LP1 = LP2 = 3.411 \mu H$, and the three coefficients of coupling were all taken equal to 0.975.

The transistors Q1 and Q2 were taken to be 2N5102's . They were simulated in SPICE by the Gummel-Poon model given below:

```
.MODEL Q5102 NPN (BF=24.8,BR=0.7,IS=9.79E-12,RE=.07,
+RC=0.1,VAF=80.4,VAR=15,ISE=1.1E-10,NE=1.46,TF=0.82NS,
+TR=200NS,CJC=261PF,VJC=.5,MJC=.388,CJE=688PF,VJE=1.
+MJE=.345,PTF=45)
```

With this model it was found that for $VCC = 24$ volts, $VBB = 0.56$ volts gave quiescent collector currents of 26.4mA with base currents of 1.12mA. The voltages VB1 and VB2 were assumed sinusoidal, 180 degree out of phase, and to have equal amplitudes. At 1 Mhz an amplitude of 0.48 volts (peak) carried both transistors to the edge of saturation .

A complete SPICE run is given in Appendix A. This run is at 1 Mhz with two changes in the 2N5102 model: both TF and CJC are halved from the values given above. The operation at 1 Mhz was not influenced significantly by this change. The

operating path for both transistors is the same except for the 180 degree phase difference. Figure 7 plots this path in the i_C-v_{CE} plain for Q1. At this frequency

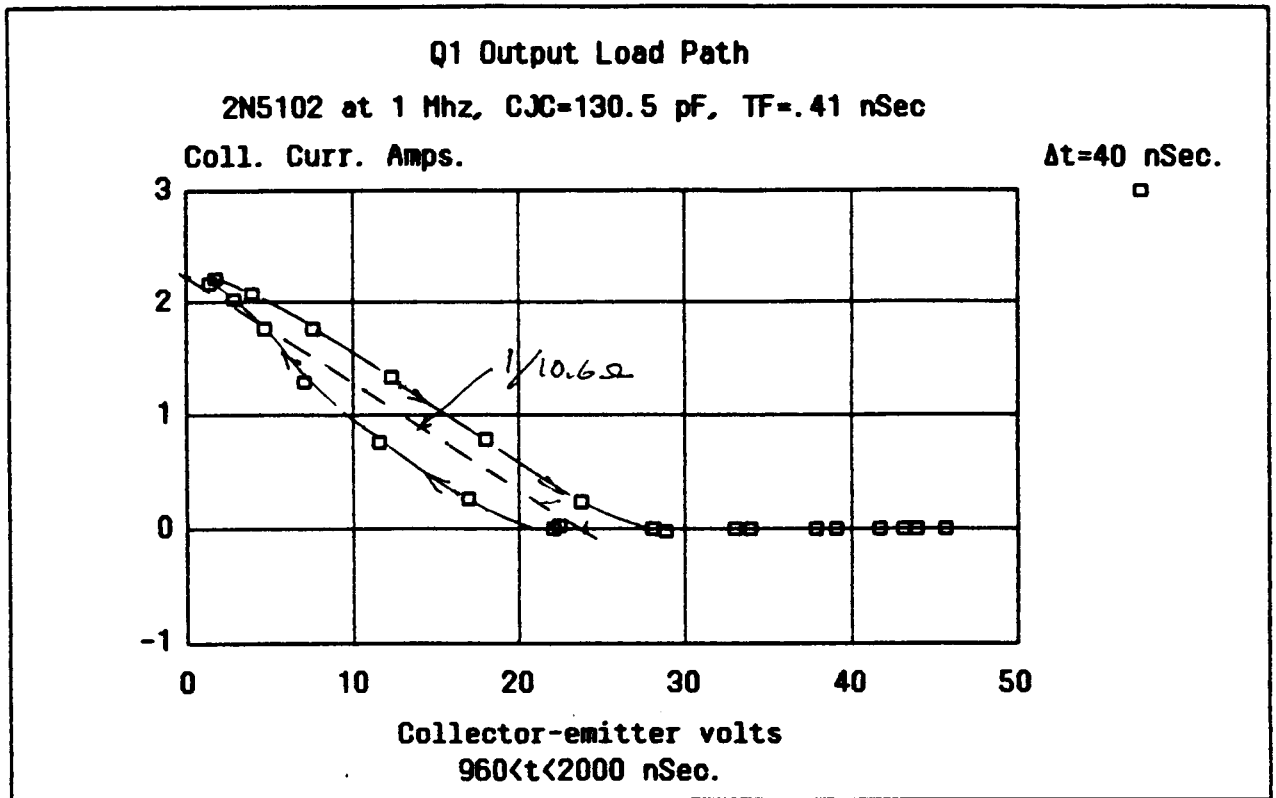


Fig.7 Q1 operating path at 1 Mhz

the load seen by Q1 is almost a pure resistance of 10.6 ohms. The peak collector current is 2.217 amperes and the minimum collector-emitter voltage is 1.447 volts. The corresponding numbers for Q2 are 2.207 amperes and 1.104 volts.

A plot of i_C^{Q1} and v_{C4} (the quadrupole voltage) versus time is shown in Fig.8.

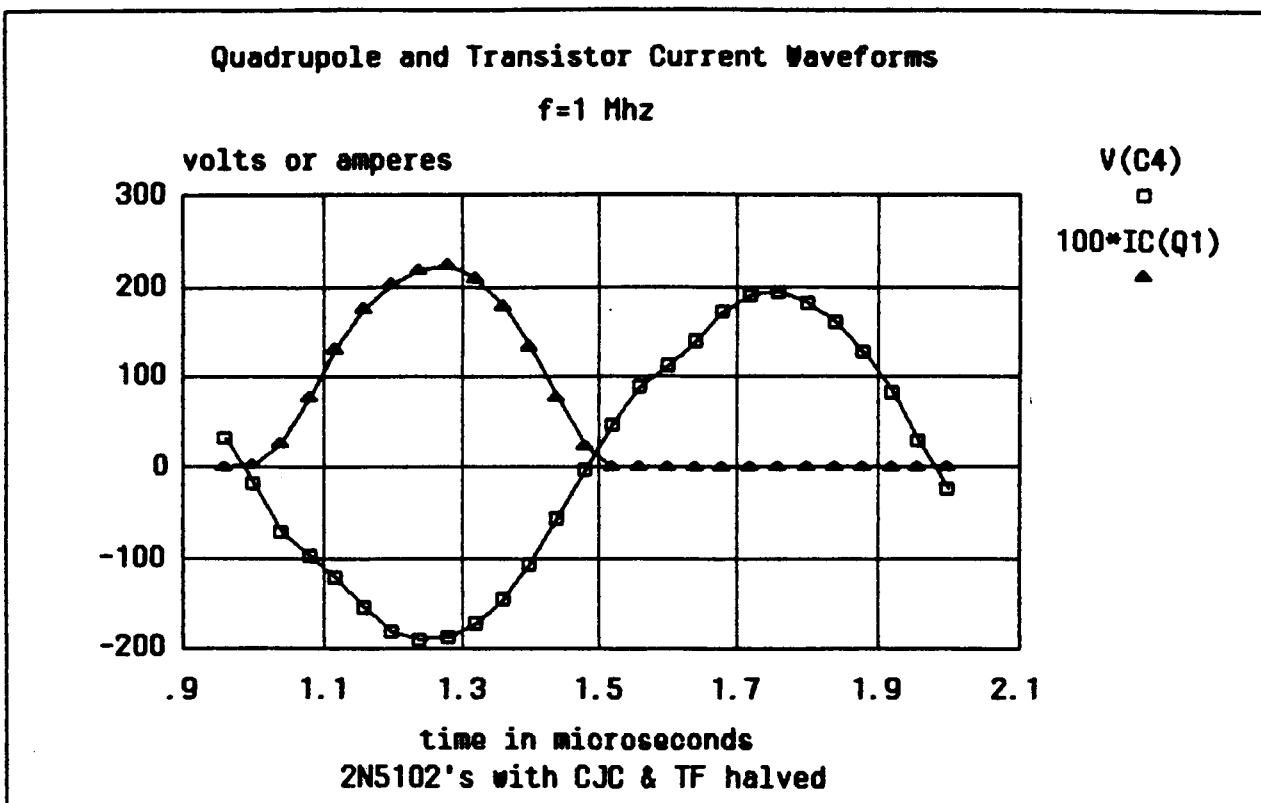


Fig.8 Calculated Quadrupole voltage and Q1 collector current waveforms.

The peak-to-peak amplitude of the quadrupole voltage (V(12) in Appendix A) is 383 volts, and the waveform is reasonably close to sinusoidal. The Fourier analysis shows there is 4.91% 3rd and 2.29% 5th harmonic, and the total harmonic distortion is 5.55%.

The average current from the VCC supply is 1.342 amperes which makes

$$P_{CC} = I_C \cdot V_{CC} = 32.2 \text{ watts.}$$

At 1 Mhz. the load impedance is almost purely resistive, and the voltage across the 42.4 ohm resistor (V(4,5) in Appendix A) is 90.5 volts p-p. The power to that resistor is therefore

$$P_{RL} = |V(4,5)|^2 / 8 \cdot R_L = 24.2 \text{ watts,}$$

and the amplifier's collector efficiency is 75.3%.

It should be noted that for this application "the load" is a 25 pF capacitance, and therefore the collector efficiency is of only secondary importance. The power supplied by VCC will always be the average of the two collector currents times twenty-four volts, and to a first approximation this will depend only on the peak values of the current waveforms. They will be approximately constant over the entire frequency range. As the input impedance varies between 0 and 10.6Ω with changing frequency, the power to RL will vary from 0 to 24.2 watts, but the input power will not change. The difference will be dissipated in the transistor collectors.

For the present example design, one can expect the transistor dissipation to vary between

$$(32.2-24.2) \div 2 = 4.0 \quad \text{and} \quad 32.2 \div 2 = 16.1 \quad \text{watts per transistor.}$$

Holding the peak input voltages constant at 0.48 volts peak, additional SPICE analyses have been run for 4, 8, 10, 12, 14, 15, and 16 megahertz. Figure 9 summarizes some of the results of these runs.

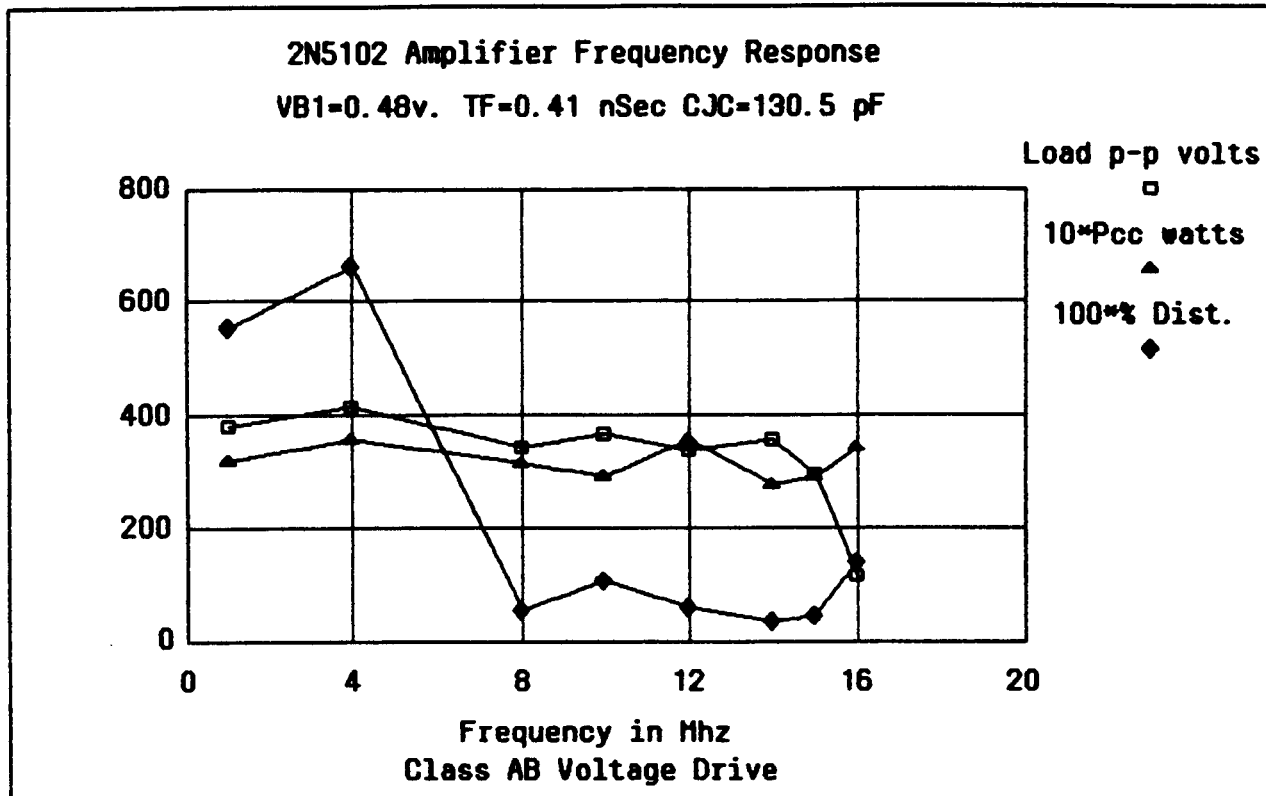


Fig.9 Output voltage, Percent distortion, and Power input versus frequency for constant input voltage.

This same data is presented in Table 1.

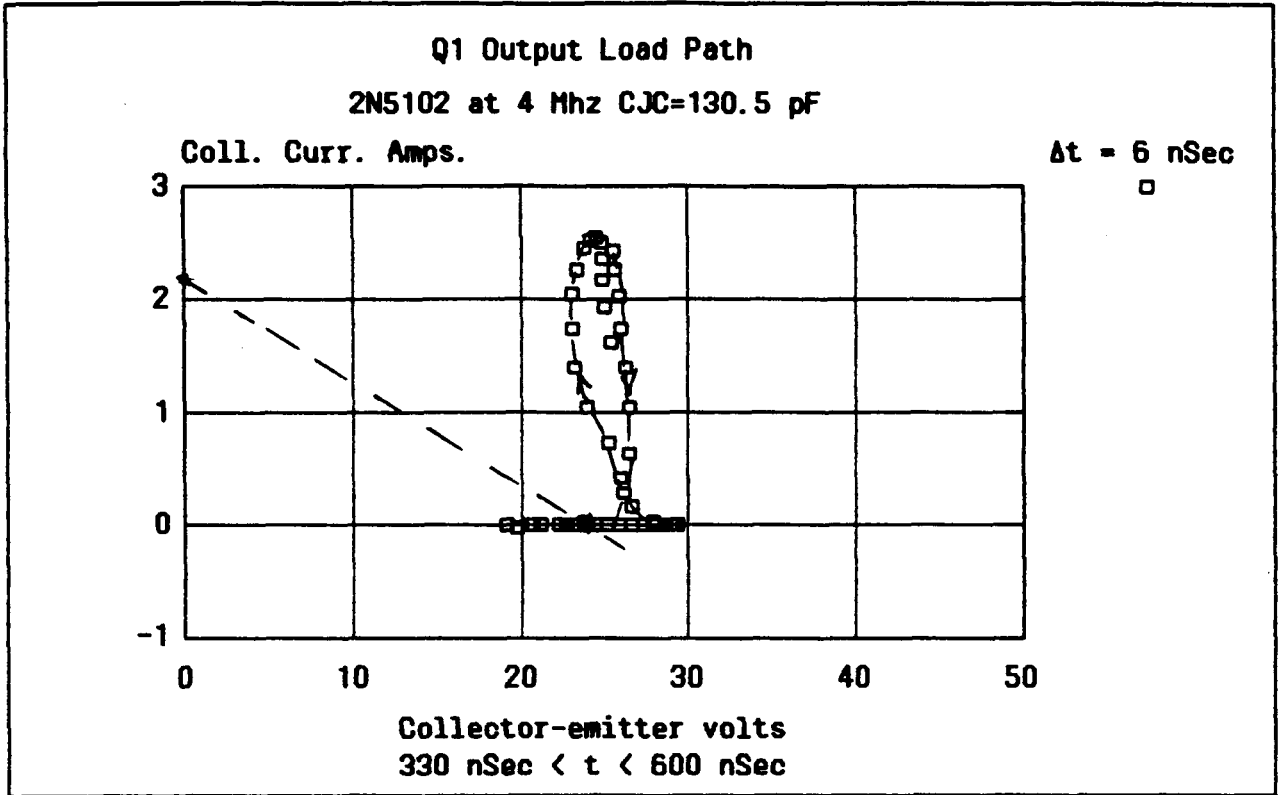
Table 1 SPICE Calculated Amplifier Performance

Freq. in Mhz	V _{C4} p-p volts	P _{CC} in watts	Percent Distortion
1.0	383	32.2	5.55
4.0	413	35.6	6.60
8.0	346	31.6	0.53
10.0	370	29.3	1.05
12.0	338	35.7	0.61
14.0	357	27.8	0.38
15.0	298	29.2	0.45
16.0	116	34.6	1.38

These calculations confirm that the d-c input power required is relatively constant over the frequency range. The quadrupole voltage is also relatively constant

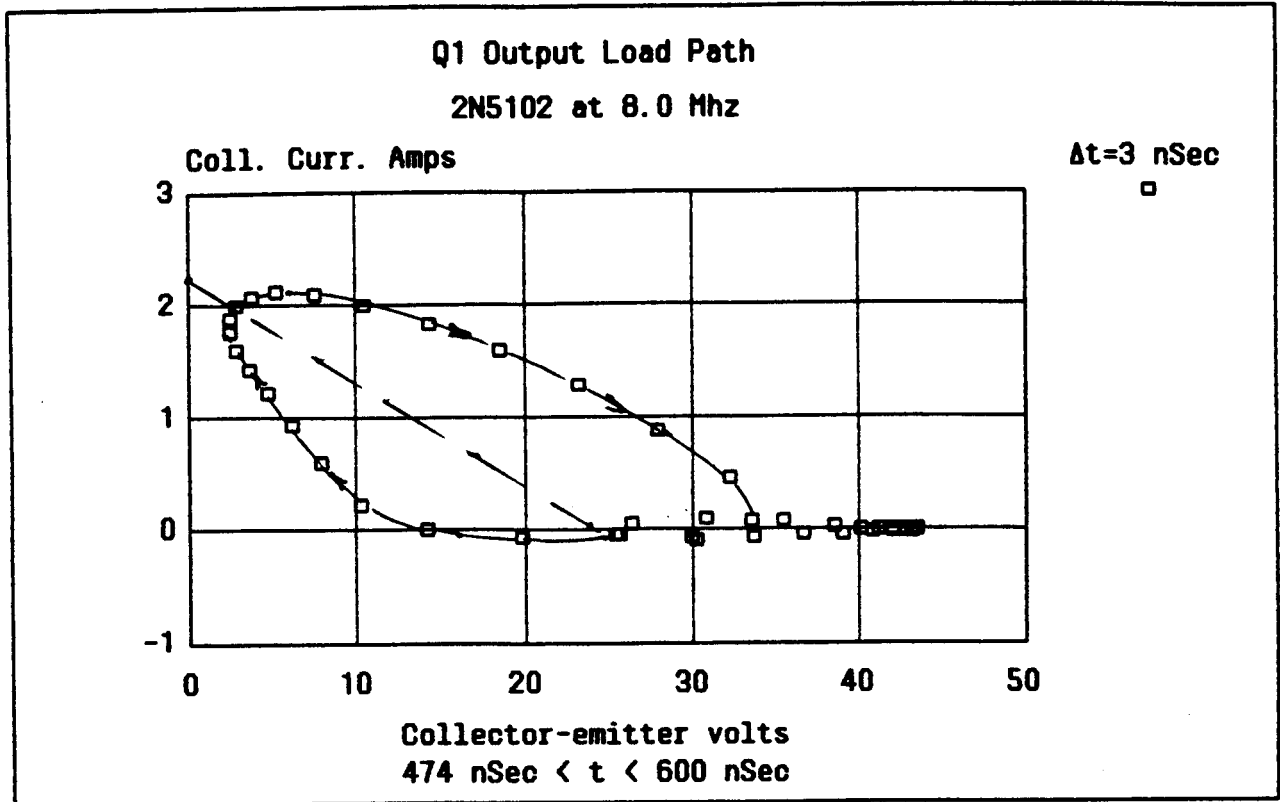
out to 15 Mhz, although less so than the coupling circuit alone (Fig.5) . This difference seems to have two causes: (1) the peak current does not stay constant because of the varying operating path at low frequencies and the transistor frequency response at the higher frequencies. (2) The leakage inductance of the three winding does not exactly match the desired inductance L_1 , and the output capacitance of the transistors does not match the n^2C_1 value.

Comparison of Figures 7 and 10(a)–(c) shows the wide variation of transistor operating path with changing input frequency . The circuit takes about

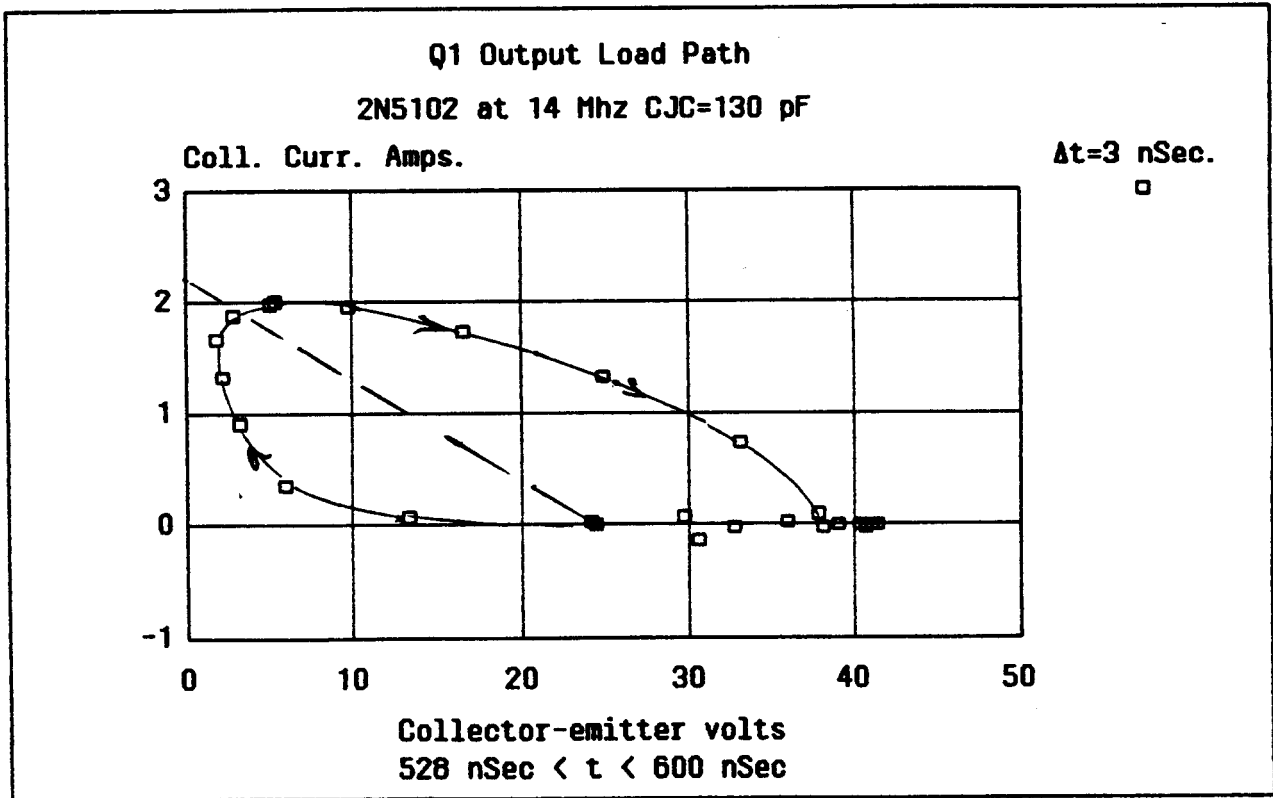


(a)

450 nanoseconds to reach steady-state operation. The plotted data is for the last cycle before 600 nSec. At 4 Mhz the transistor load is almost a short circuit, and



(b)



(c)

Fig.10 Q1 collector characteristic operating paths at (a) 4 Mhz,
(b) 8 Mhz, and (c) 14 Mhz.

the operating path is close to a vertical straight line in the i_c -VCE plain. Because of the slope of the transistor collector characteristic ($r_c \approx 65\Omega$), the vertical load line results in a significant increase in the peak collector currents at this frequency with the fixed amplitude voltage excitation. This increase contributes to the peak of voltage output and power input seen at 4 Mhz in Fig.9 . At 8 and 14 Mhz the load impedances have significant reactive components, and the drop-off in the transistor performance with increasing frequency is beginning to show.

4. Conclusions

All of the analysis and calculation confirm that it is feasible to design the amplifier and quadrupole coupling circuit needed for the Advanced Rod Control System proposed by Bruce Block. The principal system cost of the lowpass , constant amplitude rod driver amplifier is the d-c power that must be supplied. (Approximately 35 watts in the example design). This amplifier input power is constant over the frequency range and is the average power given by Eq.(6) divided by the amplifier efficiency. For sinusoidal waveforms and the lowpass coupling circuit it is not easy to exceed the efficiency of an ideal Class B amplifier, $\pi/4$. Therefore the key equation becomes

$$P_{CC} > (2/\pi) * |V_{qpole}|^2 * f_{max} * C_{qpole} \quad (10)$$

where for P_{CC} in watts

$|V_{qpole}|$ is peak-to-peak volts

f_{max} is in Hertz, and

C_{qpole} is in farads.

Circuit losses, class AB operation, and transistor limitations all will increase the power required, but with carefull design probably by not more than 20 percent.

Reducing the required quadrupole voltage will have the greatest effect on the needed d-c power. It should be borne in mind however, that Eq.(10) assumes that the system is designed for optimum performance with the selected voltage, frequency, and capacitance parameters. For a given design, assuming class B operation, reducing the quadrupole voltage by reducing the input signal amplitude will only give a linear reduction of P_{CC} with $|V_{qpole}|$.

Appendix A

SPICE Analysis of Example Quadrupole Amplifier Design

```

>*****08-13-86 ***** SPICE 26.6 3/15/83 *****15:44:09*****
>
>2N5102, 1 MHZ, VB1=0.48, TF=0.41NS, CJC=130.5PF
>
>***** INPUT LISTING TEMPERATURE = 27.000 DEG C
>
>*****
>
>
>VC1 04 08 DC 0.
>VC2 05 09 DC 0.
>VB1 02 01 SIN(0 0.48 1MEG)
>VB2 01 03 SIN(0 0.48 1MEG)
>VBB 01 00 DC 0.56
>VCC 06 00 DC 24.
>Q1 08 02 00 Q5102
>Q2 09 03 00 Q5102
>RL 04 05 42.4
>LS 10 00 216.UH
>K13 LP1 LS 0.975
>K23 LP2 LS 0.975
>C2 10 00 29.21PF
>L2 10 11 12.51UH
>C3 11 00 30.83PF
>L3 11 12 12.42UH
>C4 12 00 25.0PF
>LP1 04 06 3.411UH
>LP2 06 05 3.411UH
>K12 LP1 LP2 0.975
>.OPT LIST NDMOD
>.OP
>.WIDTH OUT=80
>.TRAN 40NS 2000NS
>.MODEL Q5102 NPN (BF=24.8, BR=0.7, IS=9.79E-12, RB=2., RE=0.07,
>+RC=0.1, VAF=80.4, VAR=15, ISE=1.1E-10, NE=1.46, TF=0.41NS, TR=200NS,
>+CJC=130.5PF, VJC=.5, MJC=.388, CJE=688PF, VJE=1., MJE=.345, PTF=45)
>.PRINT TRAN V(12) V(4) I(VB1) I(VC1)
>.PRINT TRAN V(2) V(5) I(VC2) V(4,5)
>.PLOT TRAN V(2) V(4) I(VC1) V(12)
>.FOUR 1MEG V(12) I(VC1) I(VC2) V(4)
>.END

```

*****08-13-86 ***** SPICE 26.6 3/15/83 *****15:44:09*****

>2N5102, 1 MHZ, VB1=0.48, TF=0.41NS, CJC=130.5PF

>*** SMALL SIGNAL BIAS SOLUTION TEMPERATURE = 27.000 DEG C

NODE	VOLTAGE	NODE	VOLTAGE	NODE	VOLTAGE	NODE	VOLTAGE
(1)	0.5600	(2)	0.5600	(3)	0.5600	(4)	24.0000
(5)	24.0000	(6)	24.0000	(8)	24.0000	(9)	24.0000
(10)	0.0	(11)	0.0	(12)	0.0		

VOLTAGE SOURCE CURRENTS

NAME	CURRENT
VC1	2.644E-02
VC2	2.644E-02
VB1	-1.122E-03
VB2	1.122E-03
VBB	-2.243E-03
VCC	-5.289E-02

TOTAL POWER DISSIPATION 1.27E+00 WATTS

*****08-13-86 ***** SPICE 26.6 3/15/83 *****15:44:09*****

>2N5102, 1 MHZ, VB1=0.48, TF=0.41NS, CJC=130.5PF

>*** OPERATING POINT INFORMATION TEMPERATURE = 27.000 DEG C

>*** BIPOLAR JUNCTION TRANSISTORS

	Q1	Q2
>MODEL	05102	05102
>IR	1.12E-03	1.12E-03
>IC	2.64E-02	2.64E-02
>VBE	0.560	0.560
>VBC	-23.440	-23.440
>VCE	24.000	24.000
>BETADC	23.578	23.578
>GM	1.02E+00	1.02E+00
>RPI	2.50E+01	2.50E+01
>RK	2.00E+00	2.00E+00
>RD	3.81E+03	3.81E+03
>CPI	1.33E-09	1.33E-09
>CMU	2.91E-11	2.91E-11
>CBX	0.0	0.0
>CCS	0.0	0.0
>BETAC	25.483	25.483
>FT	1.20E+08	1.20E+08

ORIGINAL PAGE IS
OF POOR QUALITY

*****08-13-86 ***** SPICE 26.6 3/15/83 *****15:44:09*****

>2N5102, 1 MHZ, VB1=0.48, TF=0.41NS, CJC=130.5PF

>**** CIRCUIT ELEMENT SUMMARY TEMPERATURE = 27.000 DEG C

>*****
>
>
>

>**** RESISTORS

NAME	NODES	VALUE	TC1	TC2
RL	4 5	4.24E+01	0.0	0.0

>**** CAPACITORS AND INDUCTORS

NAME	NODES	IN COND	VALUE
C2	10 0	0.0	2.92E-11
C3	11 0	0.0	3.08E-11
C4	12 0	0.0	2.50E-11
LS	10 0	0.0	2.16E-04
L2	10 11	0.0	1.25E-05
L3	11 12	0.0	1.24E-05
LP1	4 6	0.0	3.41E-06
LP2	6 5	0.0	3.41E-06

>**** MUTUAL INDUCTORS

NAME	COUPLED INDUCTORS	VALUE
K13	LP1 LS	9.75E-01
K23	LP2 LS	9.75E-01
K12	LP1 LP2	9.75E-01

>**** INDEPENDENT SOURCES

NAME	NODES	DC VALUE	AC VALUE	AC PHASE	TRANSIENT
VC1	4 8	0.0	0.0	0.0	
VC2	5 9	0.0	0.0	0.0	
VB1	2 1	0.0	0.0	0.0	SIN
				OFFSET.....	0.0
				AMPLITUDE....	4.80E-01
				FREQUENCY....	1.00E+06
				DELAY.....	0.0
				THETA.....	0.0
VB2	1 3	0.0	0.0	0.0	SIN
				OFFSET.....	0.0
				AMPLITUDE....	4.80E-01
				FREQUENCY....	1.00E+06
				DELAY.....	0.0
				THETA.....	0.0
VBR	1 0	5.60E-01	0.0	0.0	
VCC	6 0	2.40E+01	0.0	0.0	

>**** BIPOLAR JUNCTION TRANSISTORS

NAME	C	B	E	S	MODEL	AREA
Q1	8	2	0	0	Q5102	1.000
Q2	9	3	0	0	Q5102	1.000

>*****08-13-86 ***** SPICE 26.6 3/15/83 *****15:44:09*****

>2N5102, 1 MHZ, VB1=0.49, TF=0.41NS, CJC=130.5PF

>**** TRANSIENT ANALYSIS TEMPERATURE = 27.000 DEG C

>*****

TIME	V(12)	V(4)	I(VB1)	I(VC1)
>X				
> 0.0	0.0	2.400E+01	-1.122E-03	2.644E-02
> 4.000E-08	-2.051E-01	2.192E+01	-1.926E-02	2.932E-01
> 8.000E-08	-1.050E+01	1.903E+01	-4.099E-02	8.459E-01
> 1.200E-07	-4.655E+01	1.625E+01	-6.207E-02	1.403E+00
> 1.600E-07	-8.991E+01	1.319E+01	-7.972E-02	1.837E+00
> 2.000E-07	-1.240E+02	1.005E+01	-9.214E-02	2.125E+00
> 2.400E-07	-1.446E+02	7.735E+00	-9.725E-02	2.267E+00
> 2.800E-07	-1.485E+02	7.251E+00	-9.351E-02	2.264E+00
> 3.200E-07	-1.367E+02	8.631E+00	-8.204E-02	2.109E+00
> 3.600E-07	-1.124E+02	1.161E+01	-6.412E-02	1.798E+00
> 4.000E-07	-7.685E+01	1.605E+01	-4.167E-02	1.349E+00
> 4.400E-07	-3.162E+01	2.147E+01	-1.799E-02	7.918E-01
> 4.800E-07	1.914E+01	2.669E+01	8.332E-05	2.638E-01
> 5.200E-07	6.818E+01	3.062E+01	3.958E-03	3.195E-02
> 5.600E-07	1.059E+02	3.532E+01	6.301E-03	4.505E-03
> 6.000E-07	1.298E+02	3.977E+01	1.835E-03	-1.145E-04
> 6.400E-07	1.518E+02	4.352E+01	5.019E-03	3.719E-03
> 6.800E-07	1.814E+02	4.539E+01	2.734E-03	2.720E-03
> 7.200E-07	1.979E+02	4.685E+01	1.187E-03	1.119E-03
> 7.600E-07	1.990E+02	4.739E+01	-2.763E-04	-1.899E-04
> 8.000E-07	1.864E+02	4.677E+01	-1.082E-03	-4.419E-04
> 8.400E-07	1.642E+02	4.381E+01	-4.258E-03	-3.164E-03
> 8.800E-07	1.380E+02	3.972E+01	-4.897E-03	-3.504E-03
> 9.200E-07	8.701E+01	3.482E+01	-5.329E-03	-4.247E-03
> 9.600E-07	3.405E+01	2.899E+01	-6.738E-03	-4.114E-03
> 1.000E-06	-1.862E+01	2.255E+01	-8.989E-03	2.028E-02
> 1.040E-06	-7.018E+01	1.701E+01	-2.147E-02	2.701E-01
> 1.080E-06	-9.722E+01	1.168E+01	-4.325E-02	7.789E-01
> 1.120E-06	-1.224E+02	7.029E+00	-6.545E-02	1.297E+00
> 1.160E-06	-1.556E+02	4.661E+00	-8.276E-02	1.754E+00
> 1.200E-06	-1.803E+02	2.858E+00	-9.590E-02	2.029E+00
> 1.240E-06	-1.903E+02	1.447E+00	-1.010E-01	2.178E+00
> 1.280E-06	-1.881E+02	1.825E+00	-9.581E-02	2.217E+00
> 1.320E-06	-1.710E+02	3.979E+00	-8.359E-02	2.078E+00
> 1.360E-06	-1.451E+02	7.579E+00	-6.523E-02	1.775E+00
> 1.400E-06	-1.059E+02	1.240E+01	-4.237E-02	1.336E+00
> 1.440E-06	-5.636E+01	1.816E+01	-1.804E-02	7.860E-01
> 1.480E-06	-3.716E+00	2.390E+01	1.629E-03	2.411E-01
> 1.520E-06	4.854E+01	2.806E+01	4.529E-03	9.682E-03
> 1.560E-06	8.992E+01	3.302E+01	6.717E-03	4.768E-03
> 1.600E-06	1.144E+02	3.796E+01	4.396E-03	2.352E-03
> 1.640E-06	1.402E+02	4.184E+01	3.173E-03	1.215E-03
> 1.680E-06	1.718E+02	4.406E+01	2.063E-03	1.276E-03
> 1.720E-06	1.893E+02	4.583E+01	1.267E-03	1.340E-03
> 1.760E-06	1.928E+02	4.678E+01	1.526E-04	-8.624E-05
> 1.800E-06	1.825E+02	4.580E+01	-1.619E-03	-1.072E-03
> 1.840E-06	1.605E+02	4.322E+01	-2.947E-03	-1.913E-03
> 1.880E-06	1.282E+02	3.922E+01	-4.440E-03	-2.822E-03
> 1.920E-06	8.243E+01	3.403E+01	-5.635E-03	-3.589E-03
> 1.960E-06	3.075E+01	2.823E+01	-6.637E-03	-3.394E-03
> 2.000E-06	-2.291E+01	2.224E+01	-8.155E-03	1.086E-02
>Y				

ORIGINAL PAGE IS
OF POOR QUALITY

*****08-13-86 ***** SPICE 26.6 3/15/83 *****15:44:09*****

>2N5102, 1 MHZ, VB1=0.48, TF=0.41NS, CJC=130.5PF

>***** TRANSIENT ANALYSIS TEMPERATURE = 27.000 DEG C

>LEGEND:

>+ V(2)
>+ V(4)
>= I(VC1)
>\$ V(12)
>X

TIME	V(2)	V(4)	I(VC1)	V(12)
0.0	5.000E-01	1.000E+00	1.500E+00	2.000E+00
0.0	2.000E+01	4.000E+01	6.000E+01	8.000E+01
-1.000E+00	0.0	1.000E+00	2.000E+00	3.000E+00
-2.000E+02	-1.000E+02	0.0	1.000E+02	2.000E+02
0.0	5.600E-01	.	.	.
4.000E-08	6.793E-01	.	.	.
8.000E-08	7.909E-01	.	.	.
1.200E-07	8.876E-01	.	.	.
1.600E-07	9.623E-01	.	.	.
2.000E-07	1.013E+00	.	.	.
2.400E-07	1.036E+00	.	.	.
2.800E-07	1.028E+00	.	.	.
3.200E-07	9.911E-01	.	.	.
3.600E-07	9.271E-01	.	.	.
4.000E-07	8.400E-01	.	.	.
4.400E-07	7.353E-01	.	.	.
4.800E-07	6.196E-01	.	.	.
5.200E-07	5.002E-01	.	.	.
5.600E-07	3.845E-01	.	.	.
6.000E-07	2.781E-01	.	.	.
6.400E-07	1.910E-01	.	.	.
6.800E-07	1.269E-01	.	.	.
7.200E-07	8.853E-02	.	.	.
7.600E-07	8.109E-02	.	.	.
8.000E-07	1.040E-01	.	.	.
8.400E-07	1.550E-01	.	.	.
8.800E-07	2.324E-01	.	.	.
9.200E-07	3.292E-01	.	.	.
9.600E-07	4.409E-01	.	.	.
1.000E-06	5.600E-01	.	.	.
1.040E-06	6.791E-01	.	.	.
1.080E-06	7.910E-01	.	.	.
1.120E-06	8.878E-01	.	.	.
1.160E-06	9.643E-01	.	.	.
1.200E-06	1.015E+00	.	.	.
1.240E-06	1.038E+00	.	.	.
1.280E-06	1.031E+00	.	.	.
1.320E-06	9.932E-01	.	.	.
1.360E-06	9.287E-01	.	.	.
1.400E-06	8.415E-01	.	.	.
1.440E-06	7.364E-01	.	.	.
1.480E-06	6.201E-01	.	.	.
1.520E-06	5.001E-01	.	.	.
1.560E-06	3.837E-01	.	.	.
1.600E-06	2.789E-01	.	.	.
1.640E-06	1.910E-01	.	.	.
1.680E-06	1.272E-01	.	.	.
1.720E-06	8.885E-02	.	.	.
1.760E-06	8.100E-02	.	.	.
1.800E-06	1.044E-01	.	.	.
1.840E-06	1.551E-01	.	.	.
1.880E-06	2.328E-01	.	.	.
1.920E-06	3.306E-01	.	.	.
1.960E-06	4.416E-01	.	.	.
2.000E-06	5.600E-01	.	.	.

>Y

>*****08-13-86 ***** SPICE 26.6 3/15/83 *****15:44:09*****

>2N5102, 1 MHZ, VB1=0.48, TF=0.41NS, CJC=130.5PF

>**** FOURIER ANALYSIS TEMPERATURE = 27.000 DEG C

>FOURIER COMPONENTS OF TRANSIENT RESPONSE V(12)

>DC COMPONENT = 9.539E-01

HARMONIC NO	FREQUENCY (HZ)	FOURIER COMPONENT	NORMALIZED COMPONENT	PHASE (DEG)	NORMALIZED PHASE (DEG)
1	1.000E+06	1.897E+02	1.000000	-176.554	0.0
2	2.000E+06	5.436E-01	0.002865	9.814	186.368
3	3.000E+06	9.316E+00	0.049100	-82.602	93.952
4	4.000E+06	2.999E-01	0.001581	-38.200	138.354
5	5.000E+06	4.338E+00	0.022860	-129.934	46.620
6	6.000E+06	3.153E-01	0.001662	-95.425	81.129
7	7.000E+06	1.770E+00	0.009329	142.583	319.137
8	8.000E+06	3.725E-01	0.001963	170.410	346.964
9	9.000E+06	1.272E+00	0.006703	88.368	264.922

TOTAL HARMONIC DISTORTION = 5.552220 PERCENT

>*****08-13-86 ***** SPICE 26.6 3/15/83 *****15:44:09*****

>2N5102, 1 MHZ, VB1=0.48, TF=0.41NS, CJC=130.5PF

>**** FOURIER ANALYSIS TEMPERATURE = 27.000 DEG C

>FOURIER COMPONENTS OF TRANSIENT RESPONSE I(VC1)

>DC COMPONENT = 6.716E-01

HARMONIC NO	FREQUENCY (HZ)	FOURIER COMPONENT	NORMALIZED COMPONENT	PHASE (DEG)	NORMALIZED PHASE (DEG)
1	1.000E+06	1.078E+00	1.000000	-3.960	0.0
2	2.000E+06	5.062E-01	0.469547	-97.936	-93.976
3	3.000E+06	5.335E-02	0.049484	160.464	164.424
4	4.000E+06	8.458E-02	0.078457	-99.973	-96.013
5	5.000E+06	3.095E-02	0.028708	167.277	171.237
6	6.000E+06	1.912E-02	0.017740	-114.503	-110.543
7	7.000E+06	1.069E-02	0.009913	140.973	144.933
8	8.000E+06	8.810E-03	0.008173	-27.775	-83.815
9	9.000E+06	6.223E-03	0.005773	-170.245	-166.285

TOTAL HARMONIC DISTORTION = 48.001662 PERCENT

>*****08-13-86 ***** SPICE 26.6 3/15/83 *****15:44:09*****

>2N5102, 1 MHZ, VB1=0.48, TF=0.41NS, CJC=130.5PF

>**** FOURIER ANALYSIS TEMPERATURE = 27.000 DEG C

>FOURIER COMPONENTS OF TRANSIENT RESPONSE I(VC2)

>DC COMPONENT = 6.702E-01

HARMONIC NO	FREQUENCY (HZ)	FOURIER COMPONENT	NORMALIZED COMPONENT	PHASE (DEG)	NORMALIZED PHASE (DEG)
>					
>					
>	1	1.000E+06	1.076E+00	176.295	0.0
>	2	2.000E+06	5.065E-01	-97.954	-274.250
>	3	3.000E+06	5.493E-02	-25.249	-201.544
>	4	4.000E+06	8.508E-02	-99.251	-275.546
>	5	5.000E+06	3.085E-02	-22.299	-198.594
>	6	6.000E+06	2.050E-02	-107.070	-283.366
>	7	7.000E+06	1.205E-02	-51.167	-227.463
>	8	8.000E+06	1.139E-02	-89.874	-266.170
>	9	9.000E+06	7.964E-03	-24.050	-200.345

> TOTAL HARMONIC DISTORTION = 48.139230 PERCENT

>*****08-13-86 ***** SPICE 26.6 3/15/83 *****15:44:09*****

>2N5102, 1 MHZ, VB1=0.48, TF=0.41NS, CJC=130.5PF

>**** FOURIER ANALYSIS TEMPERATURE = 27.000 DEG C

>FOURIER COMPONENTS OF TRANSIENT RESPONSE V(4)

>DC COMPONENT = 2.412E+01

HARMONIC NO	FREQUENCY (HZ)	FOURIER COMPONENT	NORMALIZED COMPONENT	PHASE (DEG)	NORMALIZED PHASE (DEG)
>					
>					
>	1	1.000E+06	2.253E+01	-176.546	0.0
>	2	2.000E+06	4.806E-01	170.620	347.166
>	3	3.000E+06	5.067E-01	-77.218	99.328
>	4	4.000E+06	1.802E-01	173.196	349.742
>	5	5.000E+06	2.646E-01	48.056	224.603
>	6	6.000E+06	6.471E-02	142.288	318.835
>	7	7.000E+06	2.396E-01	-21.489	155.058
>	8	8.000E+06	2.747E-02	-114.198	62.349
>	9	9.000E+06	2.912E-02	-110.858	55.688

> TOTAL HARMONIC DISTORTION = 3.587558 PERCENT

> JOB CONCLUDED

> TOTAL JOB TIME 1.36

Three-Frequency Oscillator Tank Circuit

Paolo Fontani
November 10, 1987

Space Physics Research Laboratory
University of Michigan

Table of Contents

1. Introduction	1
2. Three Frequency Tank Circuit	1
2.1. Zero Placement and Pole Pre-Distortion.....	2
2.2. Foster Form.....	3
2.3. Cauer Form.....	5
3. Inductor Modeling.....	6
3.1. Implemented Inductor Model	6
3.2. Inductor Model Investigation	7
4. Conclusions	8
Appendix A.....	A-i
Appendix B.....	B-i
Appendix C.....	C-i

1. Introduction

This report presents the progress obtained so far concerning the three-frequency tank circuit to be used in the oscillator for the mass spectrometer of the CRAF project. Some interesting results have been obtained and a good solution is now visible.

At the moment the extent of the investigation is in theoretical analysis and computer simulations using the CIRAN software package. Two basic circuit forms have been examined with some positive results. Moreover, models have been investigated to represent the behavior of real inductors.

The Foster and Cauer canonical form circuits have been used to produce a three-frequency tank circuit which is of the necessary configuration for this application. Of the two, the most promising is the Foster form. Although in theory the Cauer form produces the more desirable element values it is the Foster form that results in the best component sizes when practical considerations are taken into account.

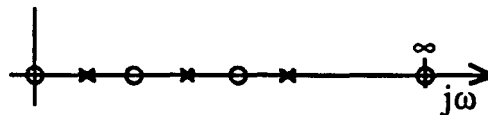
The results obtained so far indicate that the use of a three-frequency oscillator is implementable and practical. Element values are of an acceptable size (especially inductors) and impedance levels produced by the tank circuit seem to be high enough for the oscillator to operate properly.

Producing models to realistically simulate inductors and transformers is very necessary if computer simulations are to produce realistic results. This is so because these simulations have shown how critical the non-ideal characteristics of these elements are. Circuit performance is severely affected by the extent of good coupling between the primary and secondary of the transformer (ie. the value of the coupling coefficient) connecting the amplifier portion of the oscillator to the tank circuit. Additionally, the far-from-ideal nature of real inductors produce results which are distant to those obtained with ideal inductors.

2. Three Frequency Tank Circuit

Circuit synthesis has fully developed theories for the design of realizable filters and tank circuits. In a simplified manner, theory states that in order to have a realizable circuit (ie. no negatively valued elements) the poles and zeros of the circuit must alternate. For this application it is desirable to use a circuit consisting of inductors and capacitors only. This condition further constrains the pole/zero configuration to having either a pole or a zero for direct current signals (ie. frequency of 0 Hz). Additionally, since it is desired to have a DC voltage go through to the quadrupole, a zero must be selected to be placed at 0 Hz.

All of the above conditions lead to the following configuration, where "o" represents zeros and "x" represents poles:



Classical implementation of a specified pole/zero configuration involves two canonical forms, each with two variations: the Foster and Cauer forms. However, a final restriction must be considered. The input to the tank circuit is through a voltage step-up transformer while the load on it is the mass spectrometer quadrupole, which is modeled as a capacitance (of value 30 pF). In order to have a correct implementation, these elements must be taken into account as part of the Foster or Cauer form. With all characteristics considered only one Foster and one Cauer form implementation can be used.

Voltage levels and power dissipation are of concern when designing the oscillator for the mass spectrometer. The quadrupole requires high voltage levels (in the range of 400V) for the selection of certain masses. The amplifier portion of the oscillator is being designed to produce a maximum of approximately 100V. Therefore, a transformer is needed at the input of the tank circuit to step the voltage up by a factor of about four.

Since power dissipation must be kept to a minimum, the high voltage levels require the smallest possible currents. This can be accomplished by having the input impedance of the tank circuit as high as possible. One of the tank circuit design criteria thus becomes maximizing impedance levels at the operating frequencies.

The other important criterion in designing the tank circuit is to use the smallest possible inductors. This will reduce the weight and size of the oscillator, as well as avoiding possible problems in interference and unnecessary power dissipation. However, it is desirable to have a large transformer secondary inductance since this will make improved transformer performance possible.

Because of a certain tolerance in inductor sizes and impedance levels, several different tank circuits can be designed for the oscillator. This flexibility increases the possibility of designing a useful oscillator to drive the mass spectrometer quadrupole.

Three operating frequencies are needed for the mass spectrometer to have a mass selection ranging from 1 amu to 300 amu. These frequencies have been chosen to be 0.9, 1.9, and 3.75 MHz. At these frequencies the approximate voltage amplitudes (peak voltage) required are:

0.9 MHz	80 - 450 V
1.9 MHz	65 - 350 V
3.75 MHz	25 - 250 V

CIRAN was used to verify the circuit designs. This not only included verification of theory but also simulation of the circuit's performance with real elements. More specifically, the circuit had to perform correctly with real inductors and a real transformer. With this method it is possible to visualize where the circuit will not perform correctly and what measures must be taken to correct the results.

Unfortunately, CIRAN was not adequate to determine resonant frequencies and their impedance levels. CIRAN can realistically produce only a small number of points and this is usually not of high enough resolution to show the required values. In order for this to be true, approximately 1000 to 5000 points must be evaluated.

To overcome this problem, a program was written in IDL (Interactive Data Language) for use on a VAX. This program reads in the coefficients of the s-plane function produced by CIRAN and plots results of impedance magnitude and impedance phase versus frequency. Here a large number of points may be specified and an adequate resolution can be obtained. Several plots produced by this program are shown in the appendices of this document.

2.1. Zero Placement and Pole Pre-Distortion

In the design of the tank circuit only the pole locations are specified, since these are the ones that determine the resonant frequencies needed for the oscillator. On the other hand, the zeros of the circuit do not influence the value of the resonant frequencies, so they can be placed at the most convenient frequencies.

Two factors are involved in defining the convenience of a zero location: element sizes and impedance levels. The values of the elements depend heavily on the placement of the zeros. In general all inductor values tend to be large for certain combinations of zeros and very small for other combinations. Since smaller inductors are preferred in this design the zeros should be placed accordingly.

Maximization of impedance levels is also dependent on zero placement. If the zeros are placed too close to the poles, the impedance levels associated with these poles become very small. Therefore, to maximize impedance levels the zeros must be placed as far away from the poles as possible. Unfortunately, this produces larger inductors, so zero locations must be found to produce the best possible compromise.

The presence of the additional inductor (called the leakage inductor) in a non-ideal transformer model is very important. The less ideal a transformer is, the larger the leakage inductor becomes. This will adversely affect the location of the zeros in a real circuit. The zeros will shift towards the poles, reducing the impedance levels at the resonant frequencies. To correct for the shift the zeros are pre-distorted so the final effect will be the desired one. However, this pre-distortion will result in larger inductors. Therefore, a significant effort must be made to develop a good transformer.

Pole pre-distortion is necessary when an ideal circuit is implemented with real elements. This is so because real elements introduce effects that were not considered in the ideal analysis. For example, using real inductors introduces an extra capacitance corresponding to their self-capacitance. Additionally, transformers with non-ideal coupling are modeled with an additional inductor, which once again can move poles and zeros from their ideal positions.

The method used here for pole pre-distortion is an iterative one. Analysis of the ideal circuit with real elements shows how far the poles are from their desired frequencies. These differences are then added to the theoretical poles and the updated values are used to calculate new circuit values. The new element values will now place the poles closer to the desired locations but not on them. Therefore the process must be iterated several times to obtain pole positions that are satisfactory.

2.2. Foster Form

The Foster form circuit developed for our purpose is shown in Fig. 1. This is the basic form produced by the theory with an additional element (the primary inductance) to form the transformer. In theory the disadvantage of using the Foster form is that inductors L_1 and L_2 are very large. For example, for an ideal circuit with poles at 0.9, 1.9, and 3.75 MHz, and zeros at 1.35 and 2.6 MHz the element values are:

$$\begin{aligned}L_s &= 253.0 \mu\text{H} \\L_1 &= 343.0 \mu\text{H} \\L_2 &= 205.9 \mu\text{H} \\C_1 &= 40.5 \text{ pF} \\C_2 &= 18.2 \text{ pF} \\C_0 &= 30.0 \text{ pF}\end{aligned}$$

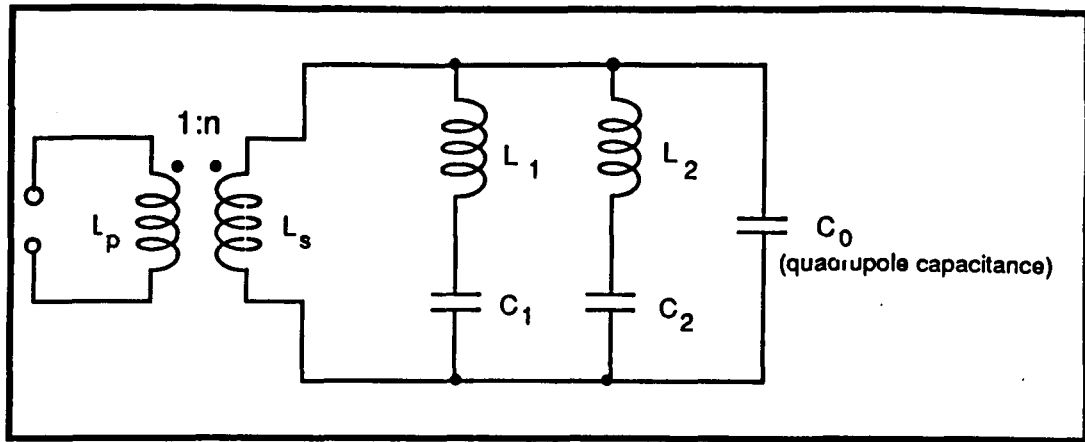


Fig. 1

The above inductors are too large for practical purposes, and only L_2 might be acceptable. However, in reality a tank circuit with these elements would not produce the required resonant frequencies. Thus, as presented in the previous section, pole pre-distortion is carried out. After several iterations a circuit is obtained which has the correct real pole positions. The final element values are:

$$\begin{aligned}
 L_s &= 109.8 \mu\text{H} \\
 L_1 &= 129.5 \mu\text{H} \\
 L_2 &= 90.7 \mu\text{H} \\
 C_1 &= 107.3 \text{ pF} \\
 C_2 &= 41.3 \text{ pF} \\
 C_0 &= 30.0 \text{ pF}
 \end{aligned}$$

These values of inductance are practical and a tank circuit can be built and used for the oscillator. A more extensive presentation of these examples, including impedance level plots, is given in Appendix A.

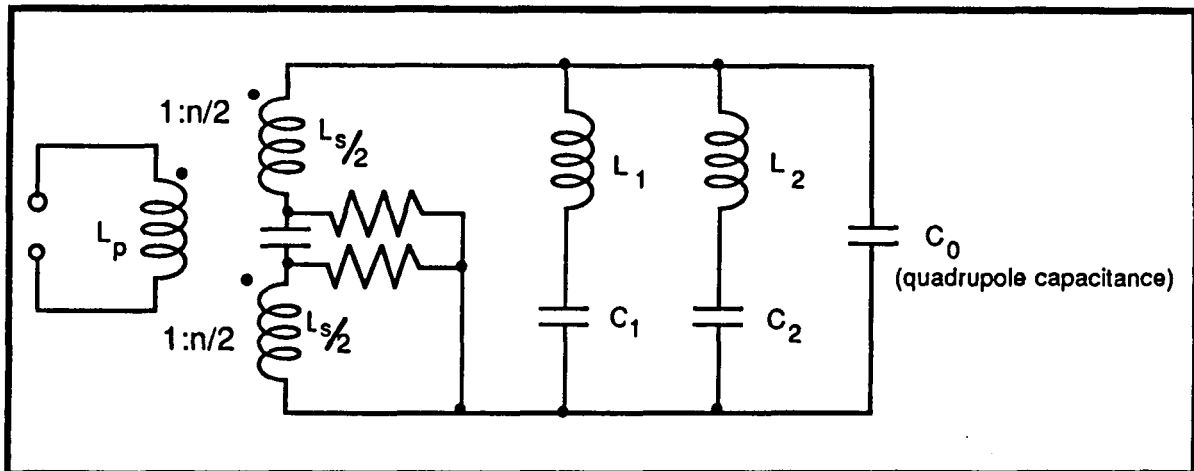


Fig. 2

Actual implementation of the Foster form tank circuit would be that shown in Fig. 2. Here the transformer's secondary inductance (L_s) is split in half and a capacitor is placed in between. This is done to create a balanced circuit in which the reference ground is present as a horizontal line bisecting the circuit. The resistors are added to create a DC path to ground for the quadrupole.

The insertion of a new capacitor between the secondary inductors will shift the poles of the circuit. For example, with a $0.1 \mu\text{F}$ capacitor the resultant poles (and their percentage deviation from the required values) are:

0.71 MHz	(-21.11%)
1.83 MHz	(-3.68%)
3.72 MHz	(-0.80%)

These results indicate that the lowest frequency must be monitored and that pole pre-distortion will have to take this new capacitor into account.

2.3. Cauer Form

Cauer form may in many respects be considered the dual of the Foster form. Its structure is different in all respects to the Foster form structure. Additionally, while Foster form theory requires large inductors, Cauer form utilizes smaller inductors. This fact makes a Cauer form tank circuit attractive for the present needs. However, as mentioned before, pole pre-distortion, to account for reality, produces inductor values that are smaller for the Foster form than for the Cauer form.

The basic Cauer form circuit needed for tank circuit implementation is shown in Fig. 3. Once again, the topography has been determined by considering the need to have L_s and C_0 as the input and output elements respectively. Fixing C_0 to 30 pF , defining poles at 0.9 , 1.9 and 3.75 MHz, and zeros at 1.3 and 3 MHz, the following element values are obtained for the ideal case:

$L_s = 188.7 \mu\text{H}$
$L_1 = 100.2 \mu\text{H}$
$L_2 = 364.7 \mu\text{H}$
$C_1 = 49.7 \text{ pF}$
$C_2 = 38.5 \text{ pF}$
$C_0 = 30.0 \text{ pF}$

Of the above values, only L_2 is impractical. Comparing these values with the theoretical values obtained for the Foster form would indicate that the Cauer form would be the best implementation of the two. However, only a comparison after pole pre-distortion can be used to choose a real circuit implementation.

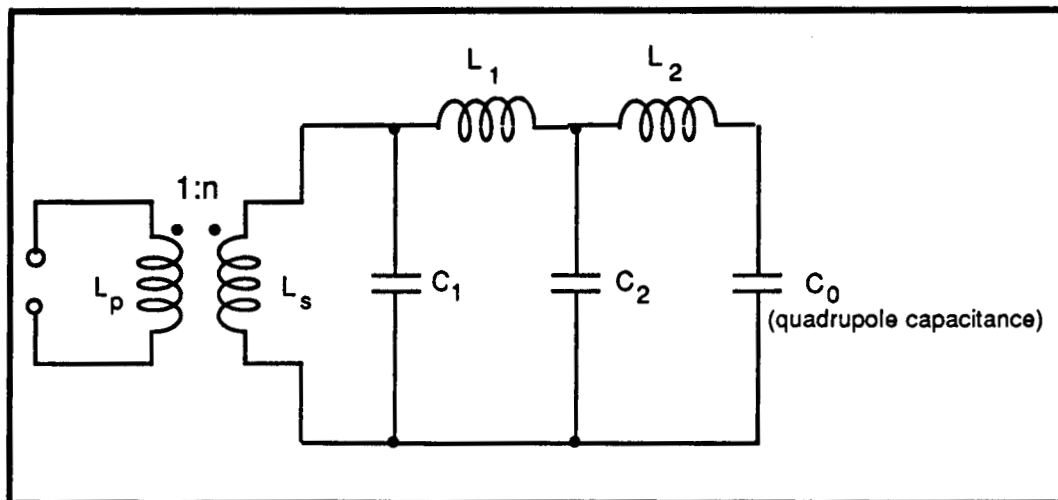


Fig. 3

When pole pre-distortion is carried out on the Cauer form the following element values result (the percentage values indicate the change with respect to the ideal circuit element values):

$$\begin{aligned}
 L_s &= 211.6 \mu\text{H} & (+12.14\%) \\
 L_1 &= 107.3 \mu\text{H} & (+7.09\%) \\
 L_2 &= 353.5 \mu\text{H} & (-3.07\%) \\
 C_1 &= 20.6 \text{ pF} \\
 C_2 &= 37.1 \text{ pF} \\
 C_0 &= 30.0 \text{ pF}
 \end{aligned}$$

Actual implementation of the Cauer form circuit requires a balanced circuit which will produce a reference ground through the middle of the tank circuit, as with the Foster form implementation. The physical circuit would then be that depicted in Fig. 4 (split transformer secondary not shown). Therefore, instead of one $107.3 \mu\text{H}$ inductor, two $53.7 \mu\text{H}$ inductors would be used, and instead of a $353.5 \mu\text{H}$ inductor, two $176.8 \mu\text{H}$ inductors.

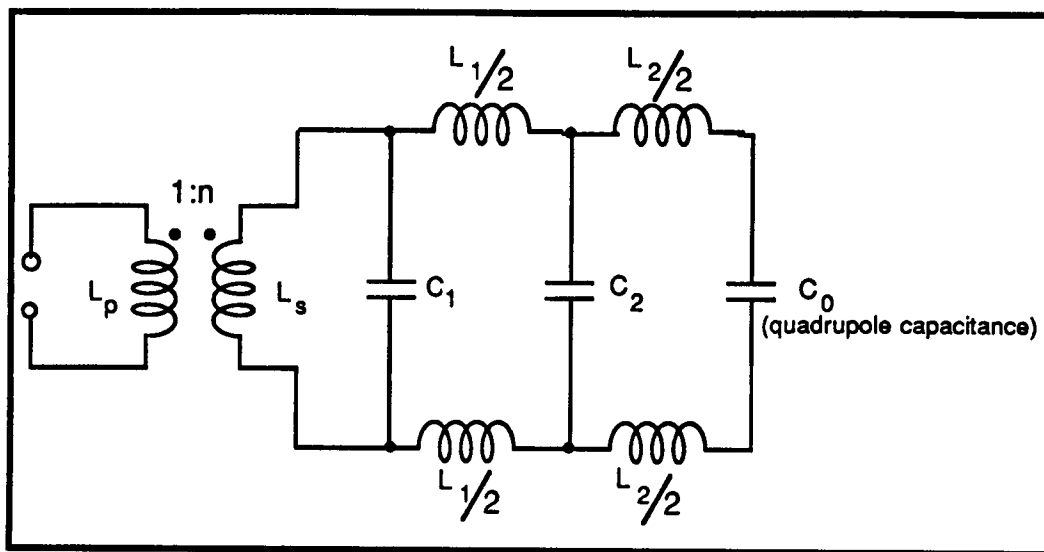


Fig. 4

Comparing the resulting Foster and Cauer circuits reveals some possible trade-offs. On the one hand, the Cauer form circuit has two inductors more than the Foster form circuit, with two of these elements being larger than the largest Foster form inductor. On the other hand, the Cauer implementation produces significantly higher impedance levels than the Foster circuit. The importance of these two factors must be taken into consideration when deciding which form will eventually be used.

3. Inductor Modeling

Since real inductors are such non-ideal elements it is necessary to develop a model using ideal elements which can closely simulate real behavior within a given frequency range. Several configurations were investigated and tested for their appropriateness, starting with a simple approach and leading to more complex circuits. One model has worked the best and is the one that is presently being used to simulate inductors in the CIRAN runs of possible tank circuits. At the moment a new model is being developed which might more closely represent real behavior.

3.1. Implemented Inductor Model

The model used to simulate inductors in present analysis is simple. It consists of four elements, as depicted in Fig. 5.

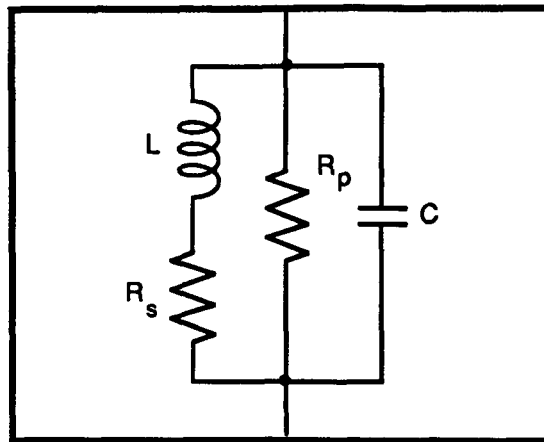


Fig. 5

In the model the capacitor represents the capacitance present between inductor windings, the resistor R_s the resistance of the wire, and the resistor R_p the core losses. The value of C can be obtained with some measurements of the inductor in question and the resistors are determined by the Q-curve of the inductor. By specifying the maximum Q and at which frequency it occurs the values can be calculated. For details on measurement requirements and equations, refer to Appendix C.

As can be apparent from the procedure to obtain the inductor model parameter values, this model has one important shortcoming. The model can accurately simulate the peak Q value at the correct frequency. However, no calculations take into consideration the Q-curve bandwidth of the inductor. As a consequence, the model bandwidth is not correct. As the frequency moves away from the peak Q the difference between model and reality becomes obvious and can be up to 50% or more.

This shortcoming makes the inductor look more ideal than it really is. Therefore real implementation will still differ significantly from computer simulations. To avoid this some more models were investigated. These models were based on the present one with extra ideal elements placed in various locations.

3.2. Inductor Model Investigation

Several different models have been investigated to replace the inaccurate model being used presently. Since the basic configuration of two conjugate-pair poles and one zero most closely resembles real inductors, no more dynamic elements can be added to the model. Therefore, the only possible additional components are resistors and sources.

Several attempts were made to add more resistors to the existing model. However, both simulation and theoretical analysis have proven that additional resistors do not improve the model's suitability.

Since extra resistors were ineffective, recent models have considered the use of dependent current sources. The reasoning behind this attempt is simple. From inductor core theory it is known that losses associated with inductors have a non-linear variation with frequency. With this in mind an attempt had to be made to have the parallel resistor vary with frequency.

No available simulation package has the possibility of defining frequency-dependent resistors, so a dependent current source was used to represent the varying resistor. As frequency changes so does the effective impedance of the inductor. This in turn affects the current going through the model's inductor. Therefore, if the current source were to depend on the current of the ideal inductor it would also vary with frequency. The proposed model is shown in Fig. 6.

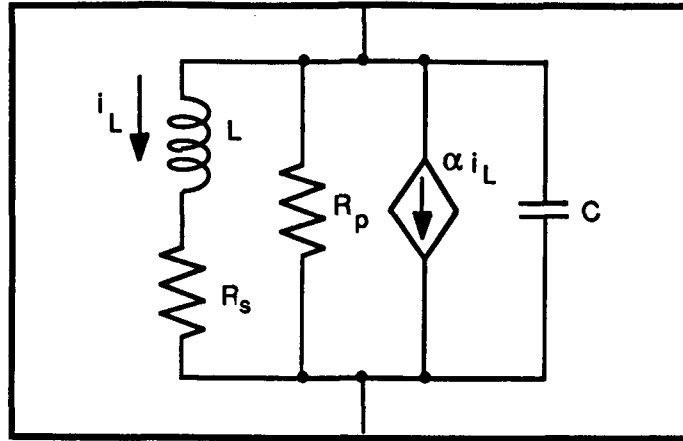


Fig. 6

This model has the effective parallel resistance increase with increasing frequency. The model's inductor current will decrease with increasing frequency. This results in the source current being smaller, which is equivalent to a larger resistance if the model's overall voltage is considered a constant.

After extensive theoretical analysis it was concluded that the above model was inadequate for our purposes. In fact, the best the model could do was have exactly the same behavior as the model being used now. A model was then chosen to reflect a "resistance" variation of the source which was opposite in nature. Instead of having the effective parallel resistance increase with frequency, the new model had the resistance decrease with frequency. This model is shown in Fig. 7.

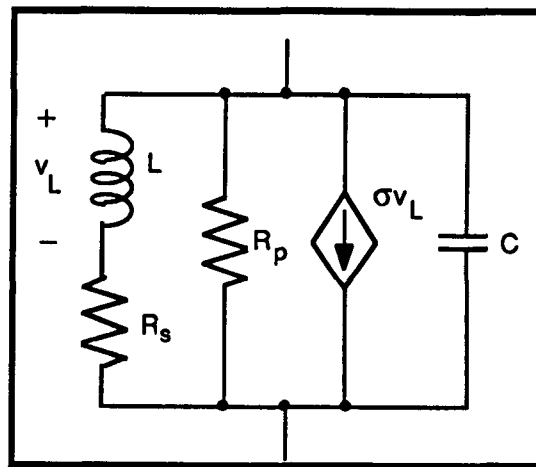


Fig. 7

While analysis of this model has not yet been completed, present results seem to indicate that this model is also inadequate for the required purposes. It should be noted here that the criterion used for judging these models is whether a set of equations can be obtained to determine the elements' values. The model itself might improve on the one being used now, but it is of few practical value if the parameters can not be calculated relatively easily.

4. Conclusions

Results from the study look promising. However, it is not know what minimum impedance levels are required to make it possible for the oscillator to work properly. Therefore, it is necessary to construct a prototype tank circuit in the laboratory which can be measured and tested in an oscillator

circuit. Fortunately, the choice of zero locations, element sizes, and impedance levels is flexible enough that variations in oscillator requirements can be met in most cases with a practical tank circuit.

Furthermore, continued attempts will be made to develop a useful inductor model with better characteristics than the one being used at the moment. It is very important that such a model be found if computer simulation is to reflect reality more closely. A possible model might use a dependent source available in one of the simulation packages of the laboratory with polynomial dependence on a current or voltage value.

Appendix A

Results of Foster Form Tank Circuit

As presented in Section 2.2, a possible Foster form tank circuit with poles at 0.9, 1.9, and 3.75 MHz has element values of:

$$\begin{aligned}L_s &= 109.8 \mu\text{H} \\L_1 &= 129.5 \mu\text{H} \\L_2 &= 90.7 \mu\text{H} \\C_1 &= 107.3 \text{ pF} \\C_2 &= 41.3 \text{ pF} \\C_0 &= 30.0 \text{ pF}\end{aligned}$$

CIRAN simulation of this circuit, using real inductors and a transformer with a coupling coefficient of 0.7, produces the results plotted on page A-iii (and a magnified plot of the 0.9 MHz frequency on page A-iv). The values printed at each peak give the frequency (in MHz) and impedance (in $k\Omega$) of the peak, for the impedance plot, and frequency, phase (in degrees) and impedance in the phase plot. The phase shift corresponding to each peak should be zero, and any variation from this value is due to the resolution of the plot.

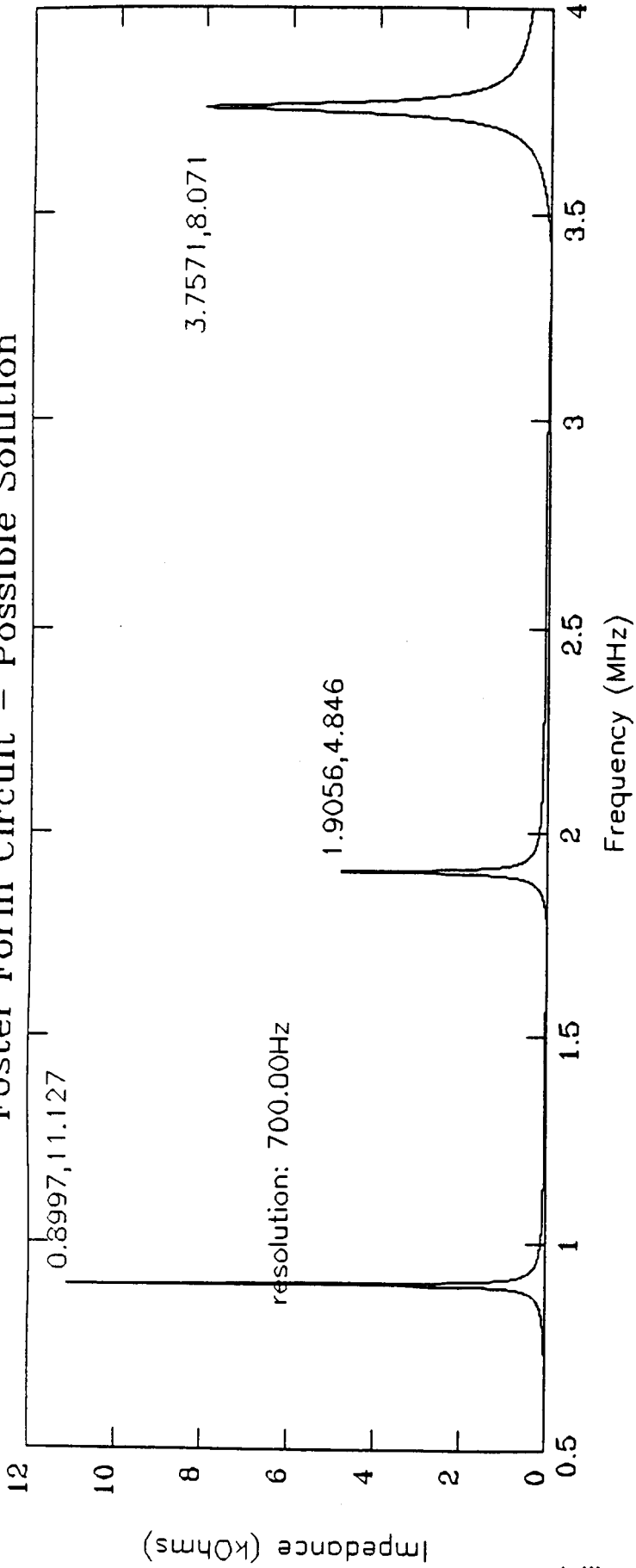
The impedance levels for the circuit are 11.1, 4.8, and 8.1 $k\Omega$ for the 0.9, 1.9, and 3.75 MHz frequencies respectively. These are assumed to be high enough for proper oscillator operation. However, an alternative solution is available. This solution has circuit element values of:

$$\begin{aligned}L_s &= 118.4 \mu\text{H} \\L_1 &= 143.4 \mu\text{H} \\L_2 &= 84.7 \mu\text{H} \\C_1 &= 96.9 \text{ pF} \\C_2 &= 41.0 \text{ pF} \\C_0 &= 30.0 \text{ pF}\end{aligned}$$

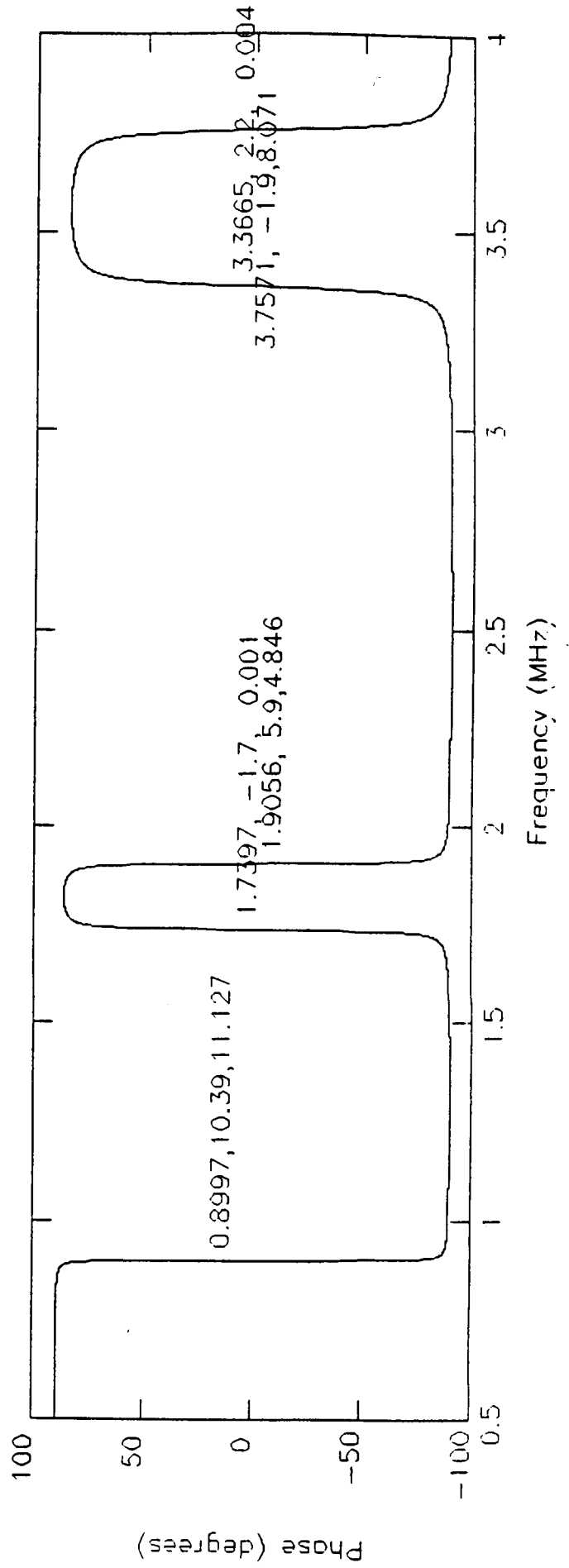
The results plot is given on page A-v and shows impedance level values of 11.6, 6.5, and 8.4 $k\Omega$. The disadvantage of this solution compared with the previous is that inductor L_1 is significantly larger, although higher impedance levels are achieved.

The second solution might not be a good substitution for the first, since impedance values are not very different, but it does show how flexible the tank circuit design can be if some allowances are made (eg. permitting larger inductor values or lower impedance levels).

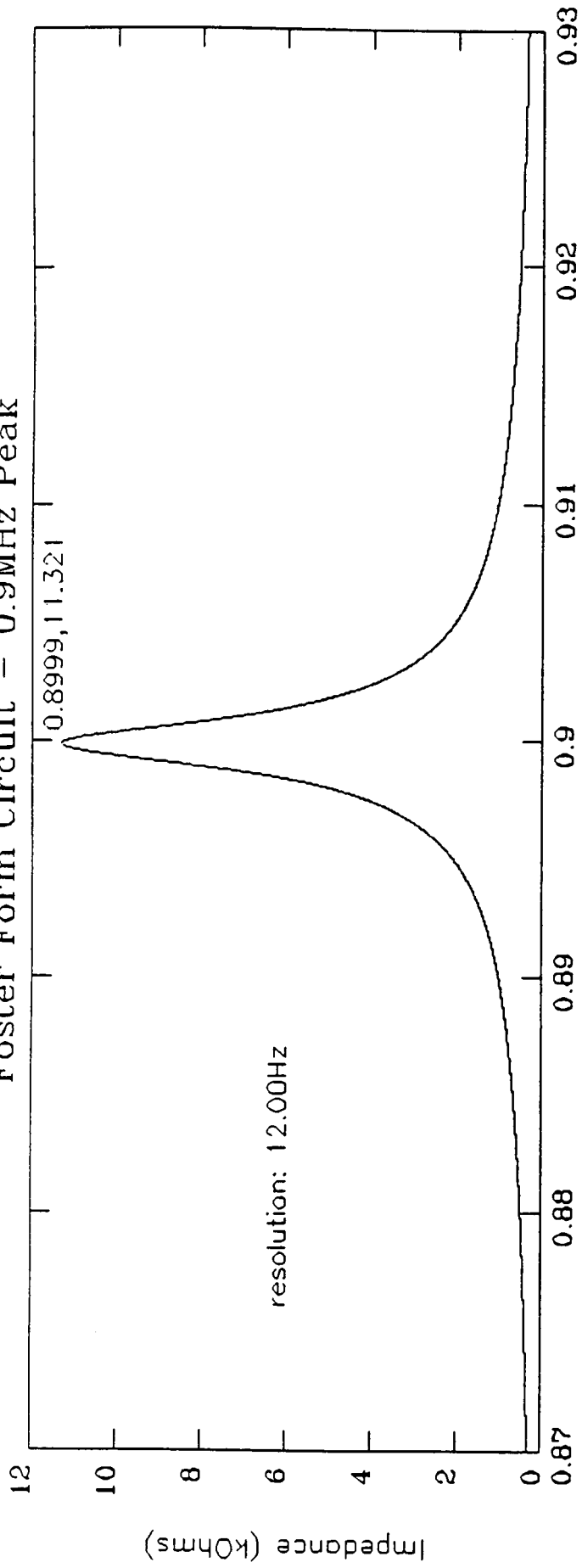
Foster Form Circuit - Possible Solution



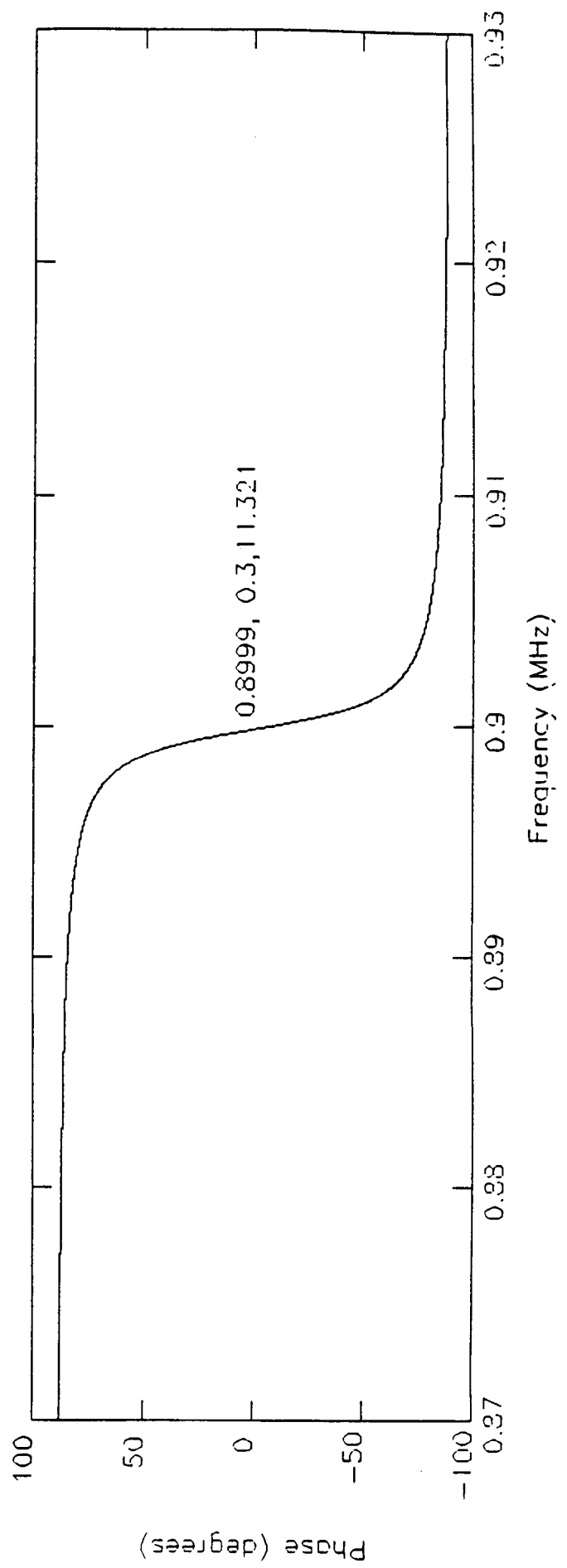
A-iii



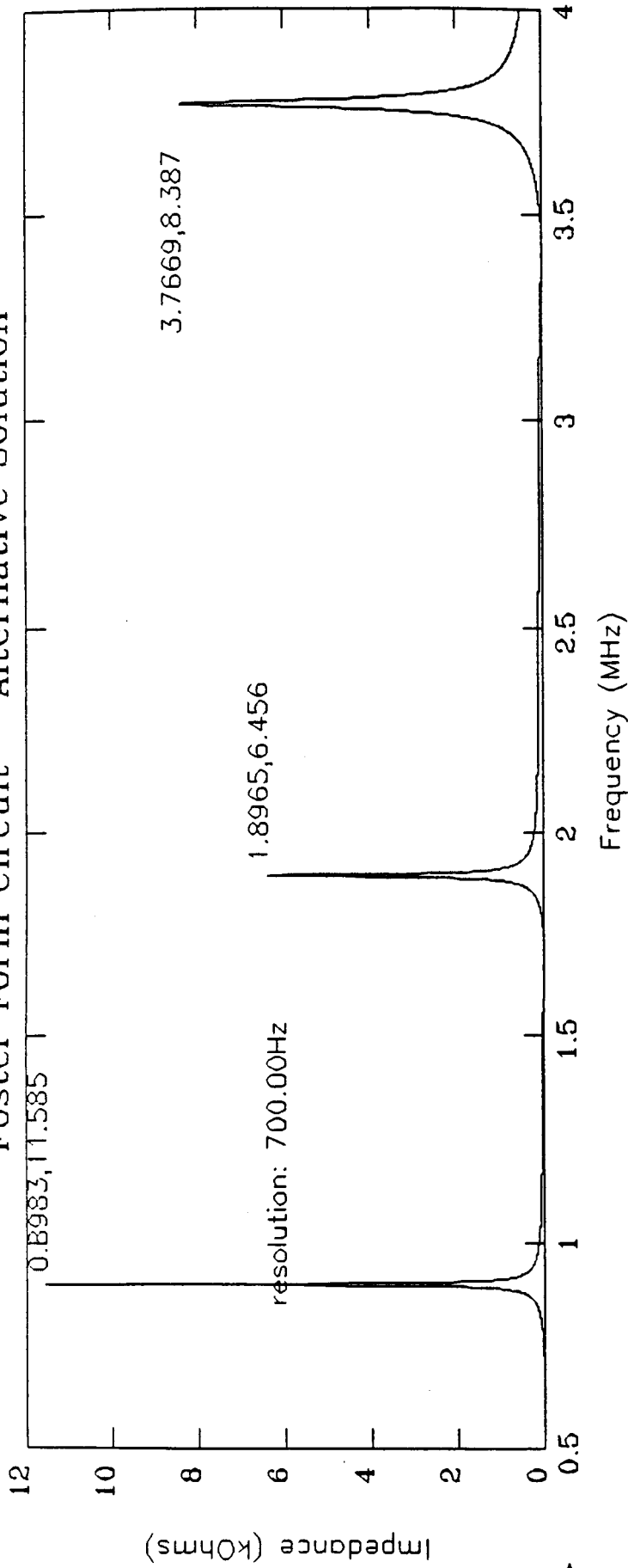
Foster Form Circuit - 0.9MHz Peak



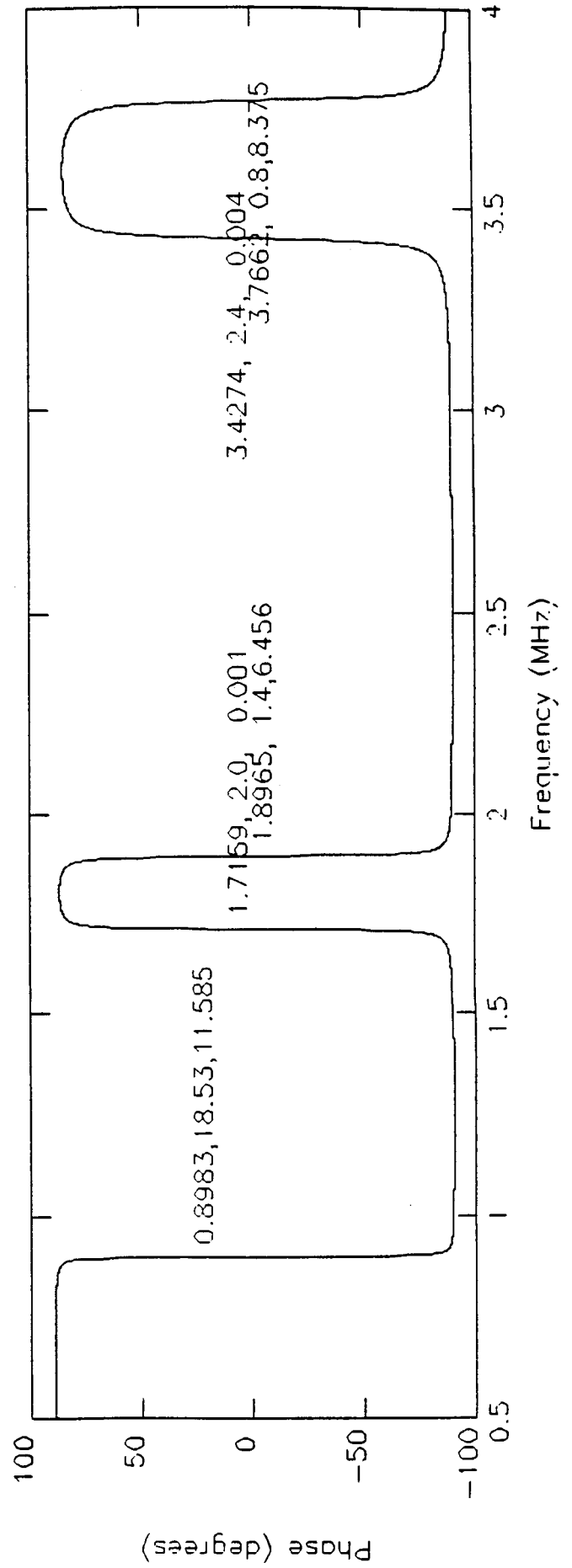
A-iv



Foster Form Circuit - Alternative Solution



A-4



Appendix B

Results of Cauer Form Tank Circuit

In this appendix, two Cauer form circuits will be presented that could be used as tank circuits for an oscillator with resonant frequencies at 0.9, 1.9, and 3.75 MHz. The difference between the two solutions emphasizes the flexibility of designing the tank circuit for this specific need. The circuit implemented and simulated is that shown in Fig. 4.

The first solution is plotted on page B-iii, which is a tank circuit with the following elements:

$$\begin{aligned}L_s &= 211.6 \mu\text{H} \\L_1 &= 107.3 \mu\text{H} \quad (53.65 \mu\text{H}) \\L_2 &= 353.5 \mu\text{H} \quad (176.75 \mu\text{H}) \\C_1 &= 20.6 \text{ pF} \\C_2 &= 37.1 \text{ pF} \\C_0 &= 30.0 \text{ pF}\end{aligned}$$

The values in parentheses are the sizes of the inductors that would actually be used in the circuit (ie. half of L_1 and L_2). This circuit produces impedance levels of 17.2, 10.2, and 11.0 k Ω for increasing resonant frequencies. These levels are higher than those of the Foster form solutions presented in Appendix A. Note, however, that the two inductors corresponding to L_2 are much larger than any in the Foster solutions.

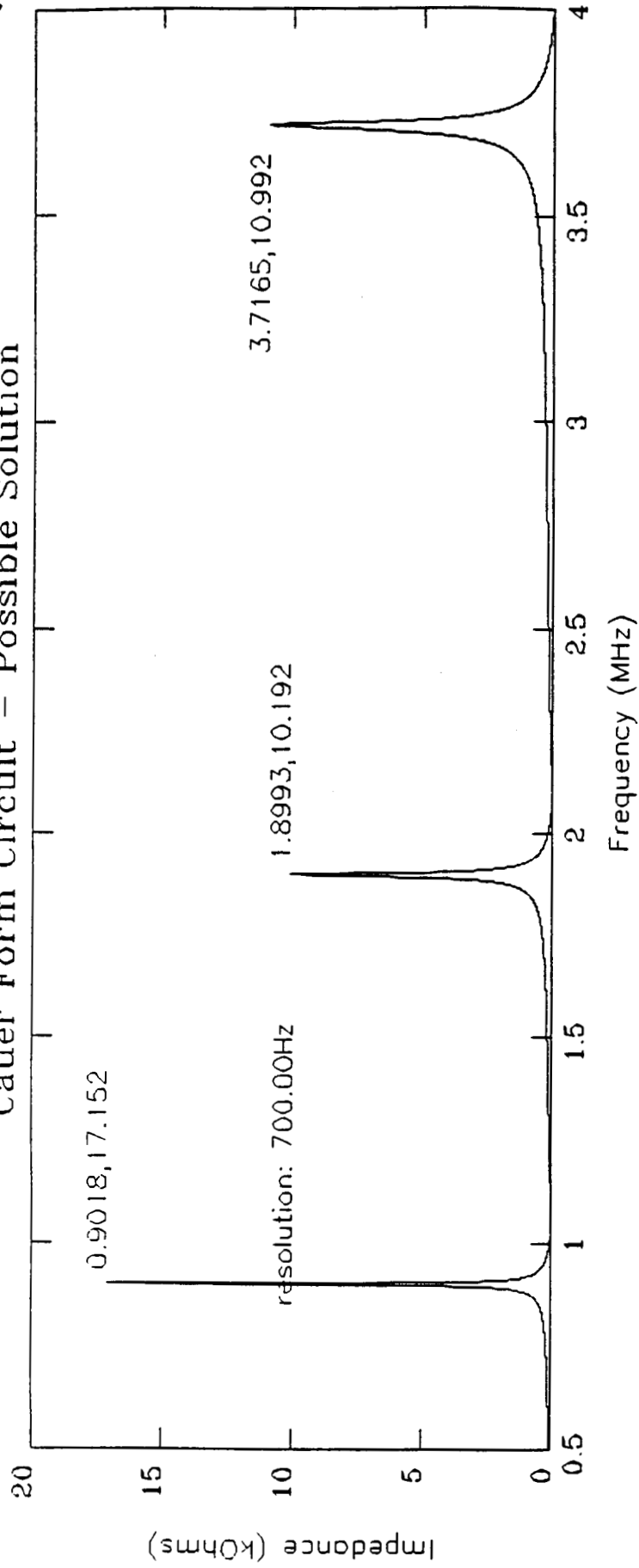
The second Cauer solution is plotted on page B-iv. Here the impedance levels are much higher than those for the previous example: 28.1, 20.5, and 24.9 k Ω . However, the element values for this circuit are:

$$\begin{aligned}L_s &= 192.7 \mu\text{H} \\L_1 &= 137.6 \mu\text{H} \quad (68.80 \mu\text{H}) \\L_2 &= 397.7 \mu\text{H} \quad (198.85 \mu\text{H}) \\C_1 &= 22.4 \text{ pF} \\C_2 &= 34.6 \text{ pF} \\C_0 &= 30.0 \text{ pF}\end{aligned}$$

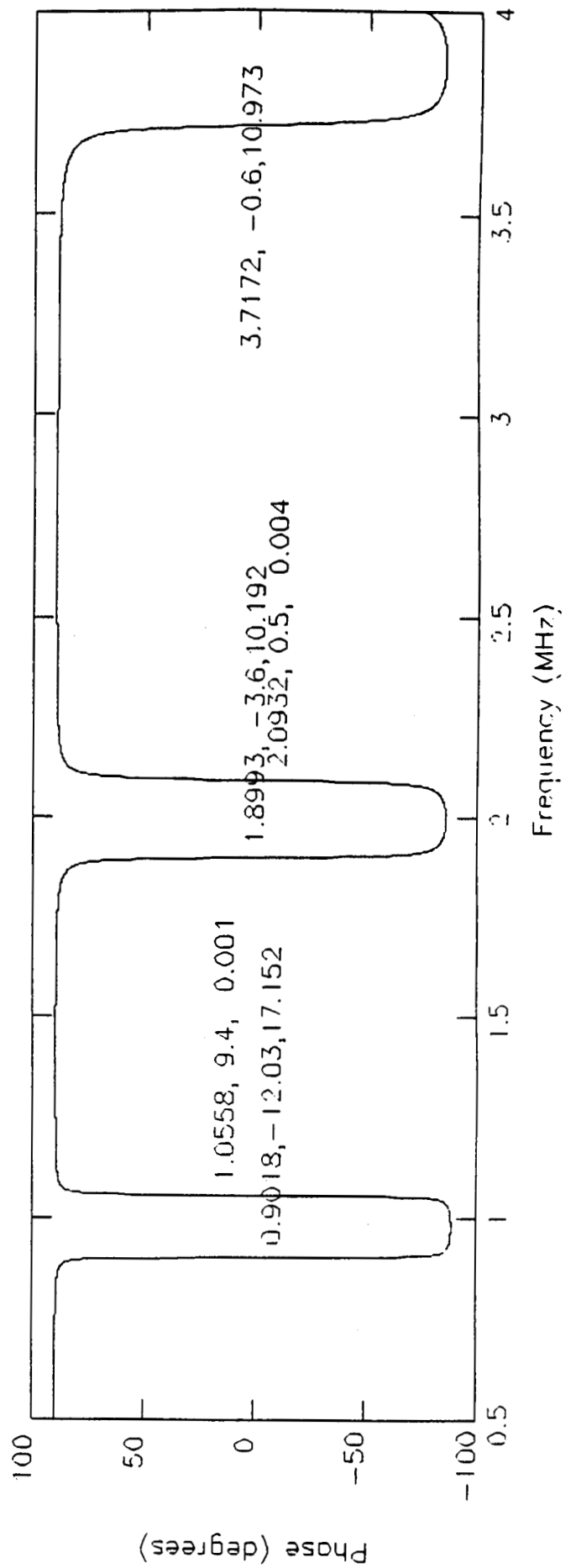
and the L_2 inductors are approaching impractical limits.

With these two solutions it is apparent that if one is willing to accept larger inductor values it is very possible to produce high impedance levels.

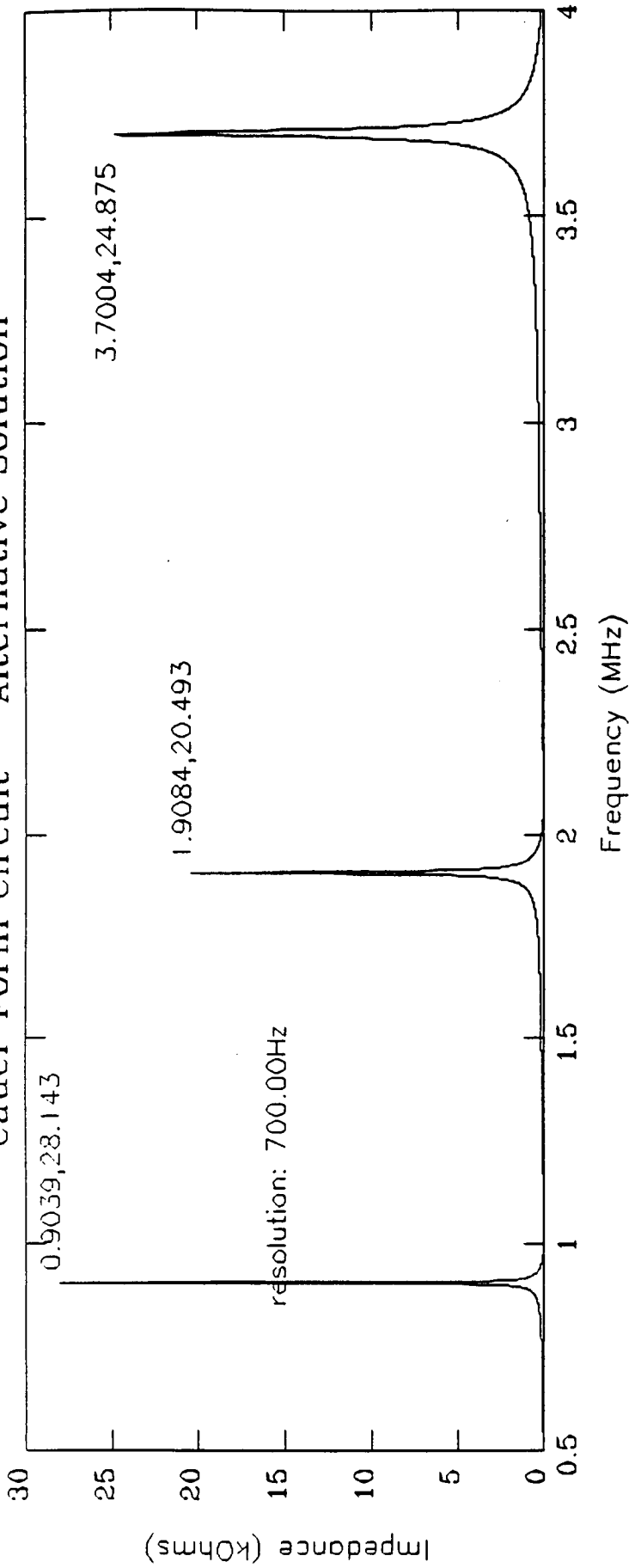
Cauer Form Circuit - Possible Solution



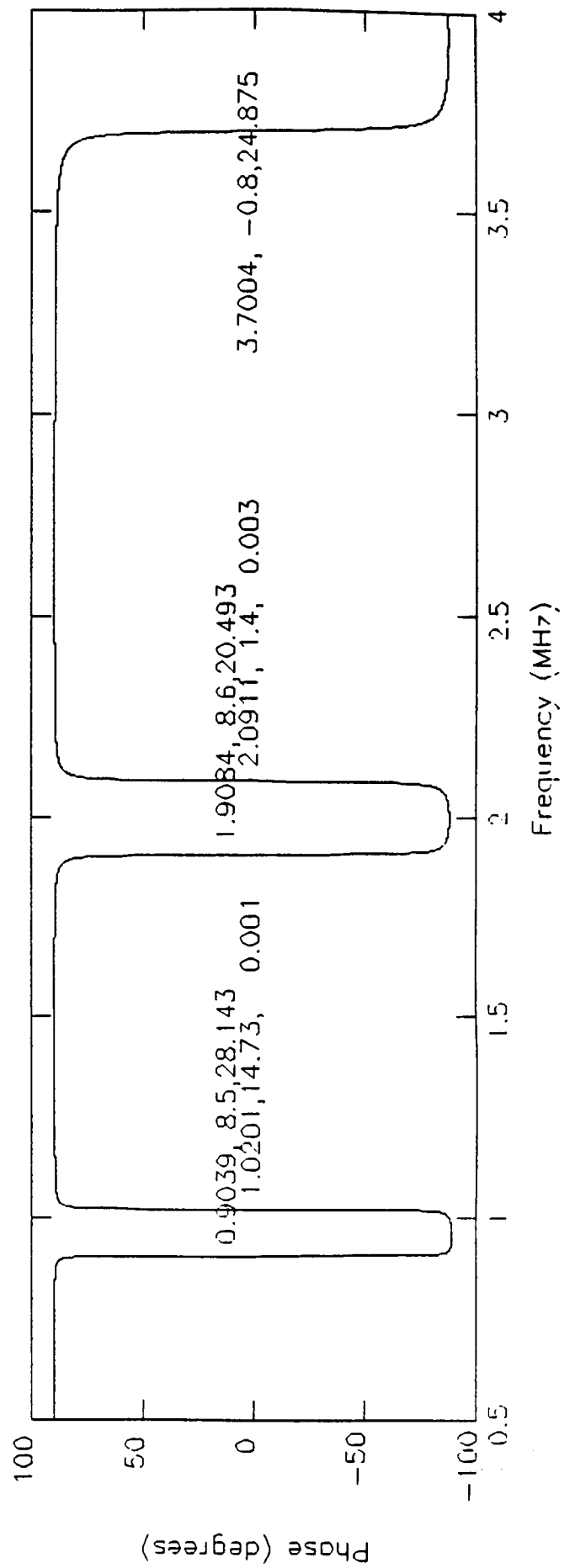
B-iii



Cauer Form Circuit - Alternative Solution



B-iv



Appendix C

Implemented Inductor Model Measurement Requirements and Equations

Of the four elements in the inductor model, two are obtained from measurements and the other two are calculated using equations obtained through theoretical analysis. The value of the ideal inductor in the model is identical to the real inductance value measured on a Q-meter. The capacitor value is obtained by extrapolation of the Q-meter data for varying frequency. It is the values of R_p and R_s that are calculated using equations.

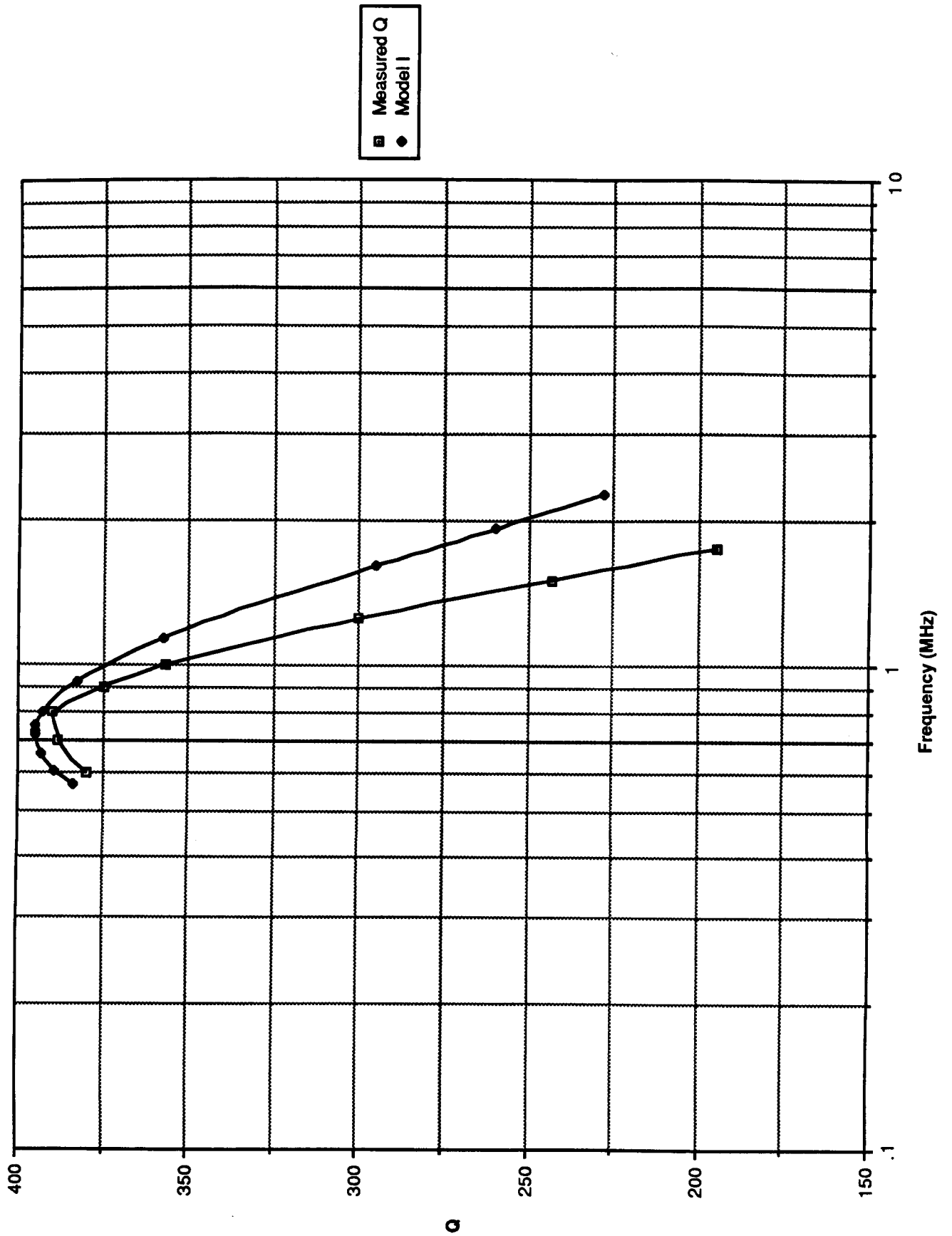
A specific phenomenon is used to obtain the value of the model capacitor. If measurements of the real inductor are made in a Q-meter it can be shown that the value of the parallel capacitance produced by the instrument to obtain peak Q at a given frequency varies linearly with the inverse of the angular frequency squared. If the data obtained is extrapolated to cross the capacitance axis a negative intercept value is obtained. The magnitude of this value corresponds to the value of capacitance inherent in the inductor.

Theoretical analysis produces simple equations to determine the values of R_p and R_s . These can be obtained by finding the peak Q value (Q_p) of the inductor in question and at which frequency it occurs (f_p). With these two values and the inductance value the following equations can be used:

$$R_s = \frac{\pi f_p L}{Q_p} \qquad R_p = 4\pi Q_p f_p L$$

With this method the model parameters are completely defined. A graph is presented on the following page showing the difference between the model performance and the actual Q-curve of a sample inductor. The peak Q values coincide, although this is not obvious from the plot since the interpolation of inductor data points is not accurate.

Comparison of Model I vs. Real Data



Measured Q
Model I